Changes in Tropical Cyclone Activity due to Global Warming in a General Circulation Model

S. Gualdi @*, E. Scoccimarro @, and A. Navarra @*

@ Istituto Nazionale di Geofisica e Vulcanologia (INGV), Bologna, Italy
* Centro Euro-Mediterraneo sui Cambiamenti Climatici (CMCC), Lecce, Italy

Corresponding author: Silvio Gualdi, V.le A.Moro 44, 40127 Bologna, Italy, gualdi@bo.ingv.it

Abstract

This study investigates the possible changes that the greenhouse global warming might generate in the characteristics of the tropical cyclones (TCs). The analysis has been performed using scenario climate simulations carried out with a fully coupled high-resolution global general circulation model. The capability of the model to reproduce a reasonably realistic TC climatology has been assessed by comparing the model results from a simulation of the 20th Century with observations. The model appears to be able to simulate tropical cyclone-like vortices with many features similar to the observed TCs. The simulated TC activity exhibits realistic geographical distribution, seasonal modulation and interannual variability, suggesting that the model is able to reproduce the major basic mechanisms that link the TC occurrence with the large scale circulation.

The results from the climate scenarios reveal a substantial general reduction of the TC frequency when the atmospheric CO2 concentration is doubled and quadrupled. The reduction appears particularly evident for the tropical North West Pacific (NWP) and North Atlantic (ATL). In the NWP the weaker TC activity seems to be associated with a reduced amount of convective instabilities. In the ATL region the weaker TC activity seems to be due to both the increased stability of the atmosphere and a stronger vertical wind shear. Despite the generally reduced TC activity, there is evidence of increased rainfall associated with the simulated cyclones. Despite the overall warming of the tropical upper ocean and the expansion of warm SSTs to the subtropics and mid-latitudes, the action of the TCs remains well confined to the tropical region and the peak of TC number remains equatorward of 20° latitude in both Hemispheres.

An extended version of this work is published on Journal of Climate (Gualdi et al. *J. of Clim*. Vol. 21, pp. 5204-5228. 2008).

1. Introduction

Tropical cyclones (TCs) are non-frontal synoptic scale low-pressure systems, which develop over warm pools of the tropical or sub-tropical oceans, with organized convection and definite cyclonic surface wind circulation (Holland 1993). A severe tropical cyclone is also known as "hurricane" in North Atlantic and North-East Pacific and "typhoon" in West Pacific. TCs are one of the most devastating natural phenomena, which often cause severe human and economic losses. Therefore, the understanding of the mechanisms that underlie their formation and evolution is a high-priority issue from both the scientific, social and economic point of view.

The increased frequency and intensity of observed hurricanes since 1995 (Goldenberg et al. 2001, Webster et al. 2005) and the extraordinary nature of the North Atlantic hurricane season that occurred in 2005 have triggered a lively discussion about the possible changes of TC frequency and intensity due to global climate change (e.g., Emanuel 2005, Trenberth 2005, Pielke et al. 2005, Anthes et al. 2006, Pielke et al. 2006., Landsea et al. 2006, among other).

A number of studies have shown that TC activity varies substantially from interannual to decadal timescales. For example, the sensitivity of the TC activity to the phase of El Niño/Southern Oscillation (ENSO) has been documented in several studies (e.g., Gray 1984, Chan 2000, Chia and Ropelewski 2002). Similarly, low-frequency modulations of the North Atlantic Oscillation (NAO) exert significant influences on the behaviour of TCs (e.g., Elsner and Kocher 2000).

The wide interannual and decadal changes, associated with natural modes of climate variability, make difficult the identification of changes in the TC features that could be unambiguously attributed to the global warming (Walsh 2004). The detection of possible trends becomes even harder when observational data-sets only are used. The destructive nature of TCs, in fact, makes the collection of observed data extremely difficult and expensive. For this reason, databases of observed TCs are available only for a few regions (particularly North Atlantic) and are generally limited in length. Furthermore, due to subjective measurements and variable procedures, reservations have been raised about the reliability of the existing tropical cyclone data-bases for estimating climatological trends (Landsea et al. 2006, Landsea 2007).

To overcome the limitations of the observational data-sets, the possible influences of global warming on TC activity also have been explored using numerical models. Since the early work of Broccoli and Manabe (1990), a number of studies have been performed both with global and regional models, reaching conflicting conclusions. Haarsma et al. (1993), for instance, found a significant increase of the number of simulated TCs in greenhouse warming experiments. However, similar simulations, but performed with higher resolution models, showed a significant reduction of the global TC activity in a warmer earth (Bengtsson et al. 1996, Sugi et al. 2002, McDonald et al. 2005, Yoshimura et al. 2006, Bengtsson et al. 2007). Royer (1998), on the other hand, found increased (decreased) TC activity in the Northern (Southern) Hemisphere, whereas Chauvin et al (2006) showed that possible changes in the frequency of TC occurrence in the North Atlantic strongly depend on the characteristics of the sea-surface temperature (SST) spatial distribution produced by the scenario simulations.

While the issue of the TC frequency response to greenhouse warming remains arguable, some consensus has been achieved about the effects on the TC intensity. Consistent with the theoretical findings of Emanuel (1987) and Holland (1997), numerous model studies, have found that the intensity of simulated TCs tends to increase in a warmer earth (e.g., Walsh and Ryan 2000, Sugi et al. 2002, Knutson and Tuleya 2004, Chauvin et al. 2006, Yoshimura et al. 2006, Oouchi et al. 2006,

Bengtsson et al. 2007). In particular, these works have shown that in a warmer climate TCs might be characterized by stronger winds and more intense precipitations. These results appear to be rather robust, as they have been obtained using a variety of models (global and regional), different resolutions and convective parametrizations. However, it is important to note that most of these studies have been conducted analyzing experiments performed with atmospheric only models forced with prescribed SSTs, thus the large majority of these experiments do not include air-sea interactions. Moreover, the SST patterns used to force the atmosphere were based on (generally low-resolution) climate scenario simulations performed with other models. This procedure, therefore, might be affected by possible inconsistencies between the simulations from which the SST patterns were taken and the atmospheric runs used to analyze the TC behaviour.

Though the air-sea feedbacks are known to be important for TC intensity (Emanuel 2003), there are only a few analysis of the TC response to global warming performed with coupled models, which, moreover, have been carried out using limited area models with simplified experimental setting (Knutson et al. 2001). On the other hand, in-depth investigations of TCs and their simulation conducted with fully coupled global models, the same as those used to perform the climate scenarios, would provide further insight into these phenomena and into our ability to reproduce and predict their behaviour.

In this study, we document the ability of a high-resolution coupled atmosphere-ocean general circulation model to simulate tropical cyclone-like vortices and explore how the features of these phenomena are possibly altered by greenhouse warming. The analysis is performed on idealized greenhouse gas forcing scenarios and a simulation of the 20° Century climate. The difference with respect to most of the previous works published on he same subject is that we use a fully coupled model, where air-sea feedbacks are accounted for.

In Section 2, a description of the model, scenario simulations and of the methodological approach used in the present paper is provided. In Section 3, we examine the ability of the model to simulate TCs. Section 4 presents an assessment of the possible changes of the TC characteristics as a consequence of global warming. In Section 5, the main findings of this work will be discussed, and the summary in Section 6 close the paper.

2. Model, Simulations and Methodology

2.1 The model

The modelling data employed in this work are time series obtained from climate simulations carried out with the SINTEX-G (SXG) coupled atmosphere-ocean general circulation model (AOGCM), which is an evolution of the SINTEX and SINTEX-F models (Gualdi et al., 2003a, 2003b; Guilyardi et al., 2003, Luo et al. 2003, Masson et al. 2005, Behera et al. 2005).

The ocean model component is the reference version 8.2 of the Ocean Parallelise (OPA; Madec et al. 1998) with the ORCA2 configuration. To avoid the singularity at the North Pole, it has been transferred to two poles located on Asia and North America. The model longitude-latitude resolution is 2° x 2° cosine(latitude) with increased meridional resolutions to 0.5° near the equator. The model has 31 vertical levels, ten of which lie in the top 100 m.

Model physics includes a free-surface configuration (Roullet and Madec 2000) and the Gent and McWilliams (1990) scheme for isopycnal mixing. Horizontal eddy viscosity coefficient in open oceans varies from 40000 m2/s in high latitudes to 2000 m2/s in the equator. Vertical eddy diffusivity and viscosity coefficients are calculated from a 1.5-order turbulent closure scheme

(Blanke and Delecluse 1993). For more details about the ocean model and its performance, readers are referred to Madec et al. (1998) or online to the web-site http://www.lodyc.jussieu.fr/opa/.

The evolution of the sea-ice is described by the LIM (Louvain-La-Neuve sea-ice model; Fichefet and Morales Maqueda, 1999), which is a thermodynamic-dynamic snow sea-ice model, with three vertical levels (one for snow and two for ice). The model allows for the presence of leads within the ice pack. Vertical and lateral growth and decay rates of the ice are obtained from prognostic energy budgets at both the bottom and surface boundaries of the snow-ice cover and in leads. When the snow load is sufficiently large to depress the snow-ice interface under the sea-water level, sea-water is supposed to infiltrate the entirety of the submerged snow and to freeze there, forming a snow ice cap. For the momentum balance, sea-ice is considered as a two-dimensional continuum in dynamical interaction with the atmosphere and ocean. The ice momentum equation is solved on the same horizontal grid as the ocean model. LIM has been thoroughly validated for both Arctic and Antarctic conditions, and has been used in a number of process studies and coupled simulations (Timmermann et al. 2005 and references therein).

The atmospheric model component is the latest version of ECHAM-4 in which the Message Passing Interface is applied to parallel computation (Roeckner et al. 1996). We adopted a horizontal resolution T106, corresponding to a gaussian grid of about 1.12° x 1.12°. In the pantheon of long coupled climate simulations, this is a considerably high horizontal resolution. A hybrid sigma-pressure vertical coordinate is used with 4-5 of a total of 19 levels lying in the planetary boundary layer. The parameterization of convection is based on the mass flux concept (Tiedtke, 1989), modified following Nordeng (1994). The Morcrette (1991) radiation scheme is used with the insertion of greenhouse gases (ghg) and a revised parameterization for the water vapour and the optical properties of clouds. A detailed discussion of the model physics and performances can be found in Roeckner et al. (1996).

The ocean and atmosphere components exchange SST, surface momentum, heat and water fluxes every 1.5 hours. The coupling and the interpolation of the coupling fields is made through the OASIS2.4 coupler (Valcke et al., 2000). No flux corrections are applied to the coupled model.

2.2 The climate scenario simulations

With respect to the previous versions of the SINTEX model, SXG includes a model of the sea-ice, which allows the production of fully coupled climate scenario experiments. In this paper, we present results obtained from the analysis of four climate simulations (Table 1).

In order to assess the capability of the model to reproduce a reasonably realistic TC activity and to evaluate the effectiveness of our TC detection methodology, the tropical cyclone-like vortices produced during the last 30 years of a 20th Century simulation have been analyzed and compared with observations. The simulation has been conducted integrating the model with forcing agents, which include greenhouse gases (CO2, CH4, N2O and CFCs) and sulfate aerosols, as specified in the protocol for the 20C3M experiment defined for the IPCC simulations (for more details see also the web-site http://www-pcmdi.llnl.gov/ipcc/about_ipcc.php). The integration starts from an equilibrium state obtained from a long coupled simulation of the pre-industrial climate, and has been conducted throughout the period 1870-2000.

Once the skill of the model to reproduce TC-like vortices has been evaluated using the present climate simulation, the possible effects induced by greenhouse global warming on the simulated TCs have been explored using 30 years of twice-daily data from climate scenario experiments. Specifically, a simulation with atmospheric CO2 concentration 287 ppm, corresponding to the pre-

industrial period (PREIND), a climate simulation with CO2 concentration doubled with respect to the PREIND period (2CO2), and a climate simulation with atmospheric CO2 concentration quadrupled with respect to the PREIND period (4CO2). The transition between PREIND and 2CO2 and between 2CO2 and 4CO2 periods has been produced by a 1%/year increment of the CO2 concentration. At the end of the two transition periods, the model has been integrated for 100 years with constant values of CO2 concentration, i.e. 574 ppm and 1148 ppm respectively.

A greenhouse warming scenario based on a doubling and a quadrupling of atmospheric CO2 is certainly an idealized experiment and does not represent a realistic forecast of future radiative forcing. The motivation of this choice resides in the fact that large concentration of atmospheric CO2 might emphasize and make more evident the response of simulated TCs to greenhouse warming. Also, the advisability of this kind of idealized experiments in the framework of TC studies has been discussed by Michaels et al. (2005) and Knutson and Tuleya (2005). Furthermore, the possible impacts of a doubling of atmospheric CO2 concentration has been explored in a number of previous works (e.g., Broccoli and Manabe 1990, Haarsma et al. 1993, Bengtsson et al. 1996, Royer 1998, Sugi et al. 2002, Knutson and Tuleya 2004, McDonald et al. 2005, Yoshimura et al. 2006, Chauvin et al. 2006), but so far no analysis has been performed on the effects of its further increase.

2.3 Reference data

The simulated TC-like vortices and the main features of their climatology are evaluated comparing the model results with observational data sets. Specifically, we use data from the National Hurricane Center (NHC) and the U.S. Joint Typhoon Warning Center (JTWC). Furthermore, the capability of the model to reproduce the observed mean climate is assessed using the ECMWF 40-year Re-Analysis (ERA40; more information available at the web-site http://www.ecmwf.int/research/era), the observational sea-surface temperature data set HadISST (Global Sea-Ice and Sea Surface Temperature Dataset produced at the Hadely Centre, Rayner et al. 2003) and the observed precipitation data set produced by Xie and Arkin (1997). For the sake of simplicity, in the rest of the paper we will refer to all of these data as observations.

2.4 Method of detection of the simulated Tropical Cyclones

Basically, two methods for detecting TCs have been commonly used in the analysis of general circulation model (GCM) experiment results. The first technique produces an estimate of the TC activity based on a genesis parameter computed from seasonal means of large scale fields (Gray 1979, Watterson et al. 1995, Royer 1998). This method has been used especially in the analysis of low-resolution model runs, as it obviates the explicit simulation of individual TCs.

The second method is the location and tracking of individual TCs based on objective criteria for the identification of specific atmospheric conditions that characterize a TC with respect to other atmospheric disturbances. In particular, TCs are identified and tracked as centres of maximum relative vorticities and minimum of surface pressure, with a warm core in high levels and maximum wind in the low layers of the atmosphere (Haarsma 1993, Bengtsson et al. 1995, Walsh 1997). In the existing literature, the definition of the criteria, i.e. the thresholds and the domain over which they are computed, varies from work to work. A discussion and a short summary for the criteria of objective TCs detection in atmospheric analysis and model simulations is given in Walsh (1997) and Chauvin et al. (2006) respectively.

In this study, we use a TC location and tracking method based on the approach defined in Bengtsson et al. (1995) and Walsh (1997). Specifically we assume that a model TC is active over a certain grid point A if the following conditions are satisfied:

- in A relative vorticity at 850 hPa is $> 3 \cdot 10^{-5}$ 1/s;
- there is a relative minimum of surface pressure and wind velocity is > 14 m/s in an area of 2.25° around A;
- wind velocity at 850 hPa is > wind velocity at 300 hPa ;
- the sum of temperature anomalies at 700, 500 and 300 hPa is > 2°K. Where the anomalies are defined as the deviation from a spatial mean computed over an area of 13 grid points in the east-west and 2 grid points in the north-south direction;
- temperature anomaly at 300 hPa is > temperature anomaly at 850 hPa ;
- the above conditions persist for a period longer than 1.5 days ;

Conditions 3, 4 and 5 distinguish TCs from other low-pressure systems and particularly the extra-tropical cyclones, which are characterized by strongest winds near the tropopause and a tropospheric cold core. The choice of the parameters in conditions 1-6 are very similar to the value indicated by Bengtsson et al. (1995) and Walsh (1997) and optimize the detection of simulated TCs in our model compared with the observations. Also, we checked the sensitivity of our results to small changes in these parameters. We found that the number of detected TCs is scarcely sensitive to the threshold values, but exhibits some sensitivity to the size of the areas over which means are computed. For a complete discussion of these criteria and their sensitivity to the parameters used the reader is addressed to Walsh (1997).

3. Simulation of the tropical climate and TC climatology

As a first step, we analyze the results obtained from a simulation of the 20th Century, as described in Section 2.2, comparing the model results with observations (re-analysis) for the period 1970-1999.

The TC occurrence has a pronounced seasonal character, with more intense activity found in the summer hemisphere (Emanuel 2003), namely in the Northern Hemisphere from June to October and in the Southern Hemisphere from December to April. Therefore, we will focus our attention on the specific seasons (and regions) of intense TC activity.

3.1 Simulation of mean state and high-frequency variability in the Tropics

Figure 1 shows the seasonal means of SST and precipitation as obtained from the observations and the model, for the extended northern summer (June-October, JJASO) and southern summer (December-April, DJFMA).

In general the model overestimates the SSTs in the tropical regions, during both seasons. The seasonal mean SST, averaged over the tropics is 0.26°C and 0.32°C warmer than observed in JJASO and in DJFMA respectively. The warm bias is visible both in the tropical Indian Ocean and Atlantic Ocean and it is particularly evident in the central-eastern Pacific, south of the equator. In this region, over the warm SSTs, the model overestimates also the rainfall, tending to produce a double ITCZ, which is a common error of most AOGCMs. In the equatorial Pacific, on the other hand, the model cold tongue is clearly too strong and extends too far west. Correspondingly, the simulated precipitation is too weak in the equatorial Pacific, especially west of the date line.

In the tropical Atlantic, the model rainfall is reasonably close to observations in JJASO, whereas during DJFMA it appears to be shifted south (by about 10° of latitude), probably as a consequence of the excessively warm SSTs found in the subtropical southern Atlantic, off the Brazilian coast. Interestingly, in the tropical Indian Ocean, the model precipitation is generally weaker than observed. During northern summer, the model shows a clear rainfall deficit in the area affected by the Asian summer monsoon, extending from the Bay of Bengal, through South-East Asia and South China Sea, up to the region east of the Philippines archipelago. Simulated precipitation appears to be too weak also over the eastern equatorial Indian Ocean, whereas it tends to be too intense in the western part of the basin, between the equator and 10°S. Also during northern winter (Figure 1, panels g and h) model rainfall is too weak over the eastern Indian Ocean and the Indonesian region.

3.2 Simulation of Tropical Cyclones

In this Section we analyze the ability of the model to simulate tropical cyclones-like vortices (that we will refer to simply as TCs), following the methodology discussed in Section 2.4. As a first step, we compare the total number of TCs per year detected in the model simulation and in the observations over the period 1970-1999 (Table 2). In general, the number of simulated TCs per year is almost 30% lower than the number detected in the observations, whereas its standard deviation is quite well captured by the model.

The geographical distribution of the TC formation positions is shown in Figure 2. In the observations (panel a) there are four distinct regions of TC formation in the Tropics of the Northern Hemisphere: North Indian Ocean (NI), West-North Pacific (WNP), East-North Pacific (ENP) and North Atlantic (ATL); and three regions in the Southern Hemisphere: Southern Indian Ocean (SI), the ocean North of Australia (AUS) and the Southern Pacific (SP). Based on these regions of TC genesis and following Camargo et al. (2004), we define seven basins (demarked by the boxes in Figure 2) that will be used to delimit and characterize the different areas of TCs activity.

The model (Figure 2, panel a) reproduces well the patterns of TCs genesis, especially in the Northern Hemisphere. The major contrast with the results obtained from the observations occurs in the southern Atlantic, where the model generates some TC, though no TCs are observed in this region during the considered period (1970-1999). This model error might be related to the too warm SSTs and intense convective activity found in this region (Figure 1). However, it is noteworthy that in March 2004 the first ever observed TC in South America, named Catarina, hit the Brazilian coast (Pezza and Simmonds, 2005).

A comparison with the results obtained with atmospheric GCMs forced with observed prescribed SSTs (Camargo et al. 2004, Figure 1) shows a substantial improvement in the patterns of TC genesis obtained with the coupled simulation. Interestingly, the comparison is made more valid by the fact that one of the atmospheric models used in Camargo et al. (Echam4) is basically the same as the one we use as atmospheric component in our coupled model. An important difference, however, is the horizontal resolution, which is T42 in Camargo et al. and T106 in our case. The enhanced model resolution might explain some of the improvements we find with our model, such as, for example, the increased global number of TCs, accompanied by a significant reduction of the number of TCs near the equator, which is a rather unrealistic feature (e.g., Camargo et al. 2004, Oouchi et al. 2006).

In Figure 3, the box plots representing the mean number of TCs per year for each area are shown both for the observations (left panel) and the model (right panel). The plots confirm that in the simulation there is a lower number of TCs, especially in the tropical North Pacific (WNP and ENP). However, in general the difference with the observations is relatively small, and, for each area, the

model simulates a fairly realistic mean year-to-year variability (see also STD in Table 2). More importantly, the simulation appears to capture the basic features of the TC distribution among the different areas. Specifically, the region with the highest mean number of TCs per year is the north-western tropical Pacific (WNP) both in the model and observations. Also the mean number of TCs in the North Indian Ocean (NI) and Atlantic region (ATL) are well reproduced, whereas the TC activity in the north-eastern Pacific (ENP) is clearly underestimated.

The results shown in Figures 1-3 indicate that the model reproduces a quite realistic tropical mean state (at least in terms of SST and precipitation) and number of simulated TC-like vortices. Furthermore, the geographic distribution of TCs appears to be in good agreement with the observations. However, so far nothing has been said about how realistic the features of the simulated TCs are.

In order to have a closer look at the structure of the model TCs, Figure 4 depicts the composite patterns of precipitation and low-level wind field obtained from the 100 most intense simulated TCs in the Northern Hemisphere. The composites were calculated by averaging the fields over the period of occurrence of the TCs and over the 100 events. The means have been computed for a domain centered on the core of the cyclones and extending 10° each side.

From these patterns it turns out that the model simulates TCs with a somewhat realistic structures. When averaged over the 100 events and their lifetimes, the mean TC has intense mean precipitation and surface winds that extend for about 300-400 Km from the centre ("eye") of the cyclone. The amplitude of the fields is substantially smaller than observed, but consistent with the results obtained from high-resolution atmospheric GCMs experiments (e. g., Bengtsson et al. 1995, Chauvin et al. 2006). In agreement with observational studies (e.g., Frank 1977, Gray 1979, Willoughby et al. 1982), the strongest wind velocities are located to the right--front sector of the core, though the maxima in the model is much too far away from the "eye". This model error is most likely due to the model resolution, which does not allow to resolve the fine and tight structures observed in "real" TCs, as suggested in McDonald et al. (2005) Chauvin et al. (2006) and shown in Bengtsson et al. (2007). For the same reason, the minimum surface pressure at the center of the storm (not shown) tends to be rather high (~990 hPa) and the simulated TC does not exhibits the "eye" in precipitation, though in general the rainfall pattern is reasonably realistic.

An important feature of the observed TCs is their marked seasonal character (Emanuel 2003). Figure 5 shows the seasonality of TC occurrence for both observations and model simulations in the Northern Hemisphere and Southern Hemisphere and for specific regions of activity described in Figure 2. In general the model reproduces well the seasonal behaviour of TCs, especially in the Southern Hemisphere, the northern Indian and Atlantic Oceans. In the Northern Hemisphere, and particularly in the North-West and North-East Pacific the annual phase of the TC activity is captured but the amplitude is much smaller, consistent with the reduced number of simulated TCs previously discussed.

Beside the seasonal modulation, the TC activity exhibits a rather strong year-to-year variability. As it has been shown in a number of studies (Gray 1984, Chan 2000, Chia and Ropelewski 2002, Frank and Young 2007, among the others), this interannual variability has a strong link with ENSO. Changes in the SST distribution in the tropical Pacific and the associated changes in the large scale circulation, in fact, appear to have a strong impact on the number of TCs that occur in different regions of the globe. The relationship between ENSO and TCs activity differs depending on the region considered.Frank and Young (2007) have shown that the number of observed TCs and the NINO3 ENSO index are negatively correlated in the North Atlantic (r=-0.55), whereas they appear to be positively correlated in the North-East Pacific (r=0.38) and Indian Ocean (r=0.24).

Figure 6 shows the interannual variation of the number of TCs in the North Atlantic, North-East Pacific and southern Indian Ocean (solid curves), along with the NINO3 SSTA index (dotted curves). Here, the value of the NINO3 index is computed for the season of maximum TC activity, i.e. JJASO for the Northern Hemisphere and DJFMA for the Southern Hemisphere. The curves shown in Figure 6 indicate that the model simulates a fairly realistic interannual modulation of the number of TCs and that this interannual variability is correlated with ENSO similarly to what is found in the observations.

All these results indicate that the model simulates intense convective disturbances with characteristics similar to the basic features of observed TCs, reassuring about its suitability to investigate how climate change might impact on the TC activity, which will be the subject of the next Section.

4. Impacts of the global warming on the tropical climate and TC climatology

Possible changes in the basic features of the tropical mean climate and of the simulated tropical cyclones due to greenhouse global warming are investigated using the climate scenario experiments PREIND, 2CO2 and 4CO2 described in Section 2.2.

4.1 Changes in the tropical mean state

The impacts of the increased atmospheric CO2 on the mean state of the Tropics is shown in Figure 7. Here the difference between 2CO2 and PREIND (2CO2-PREIND), and 4CO2 and PREIND (4CO2-PREIND) seasonal means of SST and precipitation are shown. Panels a, b, e and f indicate that the overall warming of the tropical SST is characterized by regional patterns. Both during JJASO and DJFMA, in fact, the warming is more marked in the western part of the Indian Ocean, in the equatorial Pacific and along the coast of South America, whereas a weaker warming is found in the eastern tropical Indian Ocean and eastern subtropical Pacific. In the tropical Pacific the warming patterns resemble El Niño anomalies. Interestingly, these patterns are similar for the 2CO2 PREIND and 4CO2-PREIND cases, though with different amplitudes.

Similar characteristics exhibit the patterns of difference between the PREIND, 2CO2 and 4CO2 precipitation (panels c, d, g and h). In particular, the increased CO2 induces a remarkable enhancement of precipitation along the ITCZ, from the Indian Ocean, through the Pacific to the Atlantic, during JJASO. Interestingly the increase of rainfall is confined to a relatively narrow region, very close to the equator. In the same season, areas of reduced rainfall are located in the south-eastern tropical Indian Ocean and south-central Pacific. During DJFMA, increased precipitation is found south of the equator, along the southern branch of the double ITCZ simulated by the model and discussed in Section 3.1; whereas regions of decreased rainfall are found in the subtropics of both the summer and winter hemispheres. Also in this case, the patterns of precipitation difference 2CO2-PREIND and 4CO2-PREIND exhibit very similar spatial features but different amplitudes.

Table 3 shows the changes in mean temperature, mean precipitation and mean convective precipitation over the entire globe and over the Tropics for the three experiments. Here, the convective precipitation is the precipitation associated with convective processes and produced by the convective parametrization scheme. Interestingly, while a substantial rise in mean surface temperature and mean total precipitation are found when the CO2 is increased, a completely different behaviour is found for the convective precipitation. The latter in fact shows a significant

reduction when the atmospheric CO2 concentration has doubled and quadrupled, especially in the tropical region.

A first assessment of the changes in high-frequency (< 10 days) convective variability induced by the CO2 forcing has been obtained computing the difference in standard deviation of high-pass filtered OLR anomalies (not shown). Over most of the tropical belt the sign of the difference is negative, indicating a tendency of the model to attenuate the high-frequency convective variability when the atmospheric CO2 is increased. Only over the equatorial Pacific, between about 5°N and 5°S, there is a clear sign of enhanced variability.

These results appear to suggest that increasing the concentration of CO2 in the atmosphere of the model, the general warming of the earth surface is accompanied by a reduction of the (deep) convective activity in the Tropics. The weaker convective activity, in turn, might be due to an enhancement of the vertical stability of the atmosphere. This point will be examined in more detail in Section 5.

4.2 Changes in the simulated tropical cyclones

Let us consider now what happens to the simulated TCs as a consequence of the greenhouse global warming. Table 4 shows the total number of TCs and TC days (upper row), the annual mean number of TCs and TC days (middle row) and their standard deviations (lower row) for the PREIND, 2CO2 and 4CO2 experiments. The method for detecting the TCs in these experiments is the same as the one used for the 20th century and discussed in Section 2.4. Also in this case we checked the sensitivity of the results to changes in the parameters used in the tracking procedure. In particular, we checked whether the results obtained from the 2CO2 and 4CO2 simulations might be affected by the choice of the vertical levels used to detect the warm core (700, 500 and 300 hPa). The analysis indicated that the results shown in Table 4 are scarcely sensitive to small changes in the criteria we adopted.

The results illustrated in Table 4 suggest that the total number and the annual mean number of TCs and TC days appear to be substantially reduced with increased concentration of atmospheric CO2, whereas their interannual variability does not show significant changes. Also the average duration of TC (2.7 days for the PREIND and 4CO2 experiments and 2.8 days for the 2CO2 case) does not exhibit substantial variations. Our simulations, thus, indicate that increased CO2 leads to a reduction of the TC activity, both in terms of number of TCs and number of TC days. These results are consistent with previous findings (e.g., Bengtsson et al. 1996, Sugi et al. 2002, McDonald et al. 2005, Yoshimura et al. 2006), and for the first time they have been obtained using climate scenario simulations performed with a state-of-the-art fully coupled GCM.

The box plots shown in Figure 8 represent the mean number of TCs per year for each activity area and for the three climate experiments. The reduction of the number of TCs is visible in all of the regions, though it appears to be particularly evident in the WNP and ATL areas. Interestingly, the TC activity appears to be drastically reduced also in the tropical South Atlantic (SATL).

Observational studies have hypothesized the existence of an Atlantic Multidicadal Oscillation (AMO; e.g., Delworth and Mann 2000), which modulating the Atlantic SST might influence the low-frequency variation of the TC activity in this region (Goldenberg et al. 2001). If the model produces an AMO-like variation of the SSTs and a consequent modulation of the Atlantic TC frequency, then the changes found in the TC number and shown in Figure 8 could be due to a low-frequency "natural" oscillation of the storm activity. The time series of the number of TCs in the North Atlantic have been computed for 90 years of the PREIND climate simulation and the 4CO2

experiment. In the PREIND case, the series shows a pronounced decadal variation of the TC number, apparently much more pronounced than in the 4CO2 case. However, the amplitude of the oscillation is much smaller than the differences between 4CO2 and PREIND and also during the phases of lower TC activity, the number of storms in the PREIND experiment is higher then in the 4CO2 one. Therefore, even considering the model "natural" (internal) low-frequency modulation of the TC activity, the number of TCs in the PREIND climate is systematically larger than in the 4CO2 case. This result suggests that the marked reduction of Atlantic TC number in the 4CO2 experiment is most likely ascribable to the greenhouse warming.

Generally, it is accepted that TCs tend to develop over oceanic warm waters. Specifically, climatological studies (e.g., Palmen 1948) indicate that the SST has to be warmer than about 26°C. The overall warming of the SST shown in Figure 7, implies a poleward migration of the 26°C isotherm, therefore, one could expect to find a poleward extension of the TC activity in a warmer climate.

Figure 9 shows the zonal average of the total number of simulated TCs (left panels, dashed lines) and number of TC days (right panels, dashed lines) along with the zonal mean SST (solid lines) for the three experiments, PREIND (upper panels), 2CO2 (middle panels) and 4CO2 (lower panels). In the PREIND case the zonal mean SST threshold for TC occurrence appears to be between 25 and 26°C. The maximum number of TCs and TC days occur slightly equatorward of 20° latitude in both Hemispheres.

Increasing the atmospheric CO2 (middle and lower panels) the 26°C isotherm migrates poleward, on average, of almost 10° of latitude, but the latitudinal distribution of the number of TCs and TC days do not appear to be substantially changed. The maxima of TC occurrence, though reduced, still appears to be confined equatorward of 20° latitude, and the number of TC days tends to vanish poleward of 30° latitude. On the other hand, the zonal mean SST threshold for TC occurrence increases to about 28°C and almost 30°C for the 2CO2 and 4CO2 cases respectively. These results, in agreement with previous works (e.g., Haarsma et al. 1993, Henderson-Sellers et al. 1998) suggest that the poleward migration of warm SSTs caused by the greenhouse global warming does not imply an extension of the regions of cyclogenesis or TC activities towards the middle latitudes. Similar findings for the relationship between SSTs and convective precipitation have been indicated by Dutton et al. (2000).

In order to assess possible modifications in the strength of the simulated TCs, we have analyzed the changes in intensity of both low-level winds, minimum surface pressure and precipitation associated with the model TCs. The intensity of the TC low-level wind has been analyzed using the PDI (power dissipation index) proposed by Emanuel (2005), whereas as an index of intensity of TC precipitation we consider the rainfall averaged over a 4 by 4 grid point area around the centre of the cyclone and over the duration of the event.

When the pdf (probability density function) of the PDI for the three experiments is computed and plotted (not shown), the curves do not show significant differences. Similar results are obtained from the pdf of the lowest TC minimum surface pressure (not shown). Thus, in terms of strength of the near-surface wind, the changes in atmospheric CO2 do not appear to alterate the intensity of the simulated TCs. Simulations performed with very high resolution atmospheric models, on the other hand, showed that in a warmer climate the pdf of TC intensity shifts to higher values, with a decrease of the weaker cyclones and an increment of the most intense ones (Knutson et al. 2004, Oouchi et al. 2006, Bengtsson et al. 2007). In particular, Bengtsson et al. (2007) have shown that the shift becomes more evident increasing the model horizontal resolution. We think that this shift does not occur in our simulations because of thes deficiencies that our model appears to have in

simulating intense events. It is likely, in fact, that the model produces the most intense TCs that is capable of simulating even in the PREIND climate, at least in terms of surface wind and minimum surface pressure. Therefore, the apparent lack of impact of the global warming on the simulated PDI and surface pressure, might be actually due to the difficulties of the model in representing the TC intensity, which in turn are probably ascribable to the too coarse resolution.

Different findings are obtained when we use the precipitation field to quantify the intensity of the model TCs. Figure 10 shows the pdf of precipitation (total, convective and non-convective) associated with a model TC for four different regions of activity and for the three experiments. In all of the cases, the maximum of pdf appears to shift to higher values of rainfall when the CO2 increases, indicating that in general in a warmer climate the TCs tend to be accompanied by more intense precipitation.

To further confirm these findings, in Figure 11 the composite of TC precipitation are shown. The composite represents the mean rainfall rate averaged over the TC life time and over the number of TCs for the considered regions. The means have been computed for a domain centered on the core of the cyclones and extending 5° each side. The shaded patterns show the composites of TC rainfall for the PREIND case, whereas the contours are the difference between the composite 2CO2-PREIND (upper panels) and 4CO2-PREIND (lower panels), for the WNP region (left panels) and the ATL region (right panels). Using a boot-strap technique, the changes shown in Figure 11 are found to be statistically significant, and suggest that the amount of TC rainfall, on average, becomes larger as a consequence of the greenhouse warming. These results are consistent with the findings of Knutson and Tuleya (2004), Bengtsson et al. (2007), Chauvin et al. (2006), for the Atlantic hurricanes, and Yoshimura et al. (2006), who used a high-resolution atmospheric only model.

5. Discussion

In Section 4, it has been shown that, in general, the frequency of the simulated TCs is substantially and significantly reduced when the concentration of atmospheric CO2 is increased. In order to understand this result, we discuss here how the global warming affects those characteristics of the tropical atmosphere which are of relevance for the development of the TCs. In particular, we consider the two major basic mechanisms, dynamical and thermodynamical, that can oppose the development, and hence the occurrence, of these phenomena: the vertical wind shear and the stability of the atmosphere.

It is well known that the vertical wind shear is one of the dynamical parameters that controls the formation of TCs. Specifically, strong large scale vertical wind shear represent unfavorable environmental conditions to the development of TCs (Gray 1968, Emanuel 2003). Therefore, a change in the climatological wind shear induced by greenhouse warming over a certain region might affect the TC frequency there.

Figure 12 shows the vertical wind shear for the PREIND and 4CO2 experiments and the difference 4CO2-PREIND (for the sake of brevity, we omit the 2CO2 experiment, whose results are fully consistent with the 4CO2 case, though with smaller amplitudes). Here, the wind shear is defined as the absolute value of the vector wind difference at 300 hPa and 850 hPa (i.e., winds shear =sqrt{(u_{300}-u_{850})^2+(v_{300}-v_{850})^2}). Both in the PREIND and 4CO2 case, the Tropics are characterized by a minimum of vertical wind shear, which is particularly weak in the summer hemisphere. The difference 4CO2-PREIND (bottom panels) indicates a general reduction of the wind shear over most of the Tropics. This result is in agreement with previous studies, which have shown the weakening of the tropical circulation with the increasing of the atmospheric CO2 (e. g. Knutson and Manabe 1995, Vecchi and Soden 2007a).

A notable exception is the reinforcement of the vertical wind shear in the 4CO2 experiment visible both in winter and in summer over the north tropical Atlantic. The increase of the tropical Atlantic wind shear in a warmer climate is consistent with the findings of Vecchi and Soden 2007b, and might be one of the possible causes of the TCs reduction found over this area. Interestingly, the warming patterns in the tropical Pacific SSTs found in the 4CO2 case (Figure 7) resemble the SST anomalies occurring during El Niño events. It is known that ENSO affects the TC activity over the north tropical Atlantic and one hypothesized mechanism is the modulation of the vertical wind shear strength (Goldenberg and Shapiro 1996). Therefore, the stronger response of the tropical eastern Pacific SSTs to the global warming might induce a reduction of the TC activity in the ATL region in a way (and through mechanisms) similar to the influence exerted by El Niño (see also Aiyyer and Thorncroft 2006, Latif et al. 2007).

The strengthening of the vertical wind shear, however, does not explain the reduction of the TCs over the WNP. Figure 12, in fact, shows that the wind shear reinforces over this region only during the northern winter, whereas it remains substantially unalterated in boreal summer, i.e. the TC season for this area. Therefore, there must be some other explanation for the reduced TC activity in this area.

Another important parameter that may regulate the development of TCs is the vertical stability of the atmospheric column (e.g., Gray 1979, De Maria 2001). If the atmosphere becomes more stable, the occurrence of phenomena based on the development of organized convective systems, such as TCs, becomes more unlikely. In Section 4.1, it has been shown that the increase of atmospheric CO2 is accompanied by a reduction of the convective precipitation in the Tropics. The latter, in turn, might be the sign of an increase of the vertical stability in this region. In order to investigate possible changes in the stability of the tropical troposphere, we have assessed how the Convective Available Potential Energy (CAPE) and the Convective Inhibition (CIN) (Stevens, 2005) might be affected by the greenhouse warming.

The annual mean values of CAPE and CIN have been computed for the three experiments. The results (not shown) indicate that, in general, CAPE tends to increase with the increasing of CO2 over most of the Tropics. Exceptions are found in the eastern equatorial Indian Ocean, subtropical eastern Pacific and central Atlantic, where a slight reduction of CAPE is recorded. Table 5 shows the mean value of CAPE computed over the Tropics and over the tropical oceans only. When the atmospheric CO2 concentration is doubled, on average CAPE has increased by about 20% over the Tropics and 17% over the tropical oceans, with respect to the PREIND case. The further doubling of CO2 (4CO2) leads to only a slight increase of CAPE (3% with respect to 2CO2 and 24% with respect to PREIND) in the tropical belt. However, even more interesting, over the tropical oceans, the 4CO2 CAPE increases only by about 15% compared to the PREIND value and decreases by about 2% compared to the 2CO2 case. Therefore, the increment of tropical CAPE that appears to accompany the doubling of atmospheric CO2 seems to saturate, especially over the oceans, when the CO2 concentration is further augmented.

Table 5 shows also the mean value of CIN. Similarly to CAPE, also CIN tends to increase with the CO2 concentration, and at an even greater rate. However, different from CAPE, CIN does not appear to saturate when the CO2 concentration is quadrupled. Therefore, in the model, the increased atmospheric CO2 appears to cause an increase of CAPE, i.e. an augmented conditional instability, but also an even more pronounced increment of CIN, i.e. a higher energy barrier preventing the convection from occurring spontaneously.

Figure 13 shows the pdf of the level of free convection (LFC) for the PREIND, 2CO2 and 4CO2 cases over the WNP and ATL areas. The results suggest that the LFC tends to be higher when the atmospheric CO2 concentration increases. Consistent with the larger CIN, the effects of the higher LFCs is to reduce the chance for convective instabilities to develop.

The generally larger potential energy barrier (CIN) and the shift of the LFC to higher levels, making less likely the development of convective systems, might be responsible for both the general diminishing of convective precipitation and, at least in part, for the reduced occurrence of TCs, especially in the WNP region. For the ATL region, on the other hand, the decreased number of TCs appears to be probably due to both the increased vertical wind shear and the reduced instability of the atmosphere.

Importantly, the reduction of the convective activity suggested by the results of this work is fully consistent with the findings of other studies, where the effects of atmospheric CO2 concentration on the tropical convection have been investigated (e.g., Knutson and Manabe 1995, Sugi and Yoshimura 2004, Held and Soden 2006, Vecchi and Soden 2007a).

The warming of the tropical troposphere is accompanied by an increase of water vapor, especially in the lower layers (not shown), which, in general, leads to an increase of the potential energy available for convection. In fact, as we have seen in Table 5, the tropical CAPE increases in the 2CO2 and 4CO2 experiments compared with the PREIND case. Therefore, when convection occurs it has more potential energy available and the events might be more intense. In other words, the increase of CIN makes the triggering of convective episodes more difficult, but the larger CAPE makes the convective episodes stronger. This might explain the increased intensity of TC precipitation, found in Section 4.2 (Figure 10 and Figure 11).

In order to further substantiate our findings, we have assessed how other (empirical) indices related to the TC activity are changed as a consequence of the greenhouse warming. Specifically, parameters like the mid-tropospheric relative humidity over the oceans, the maximum potential index (MPI, Bister and Emanuel 2002) and the genesis potential (GP) index (Emanuel and Nolan, 2004) have been found to be related with the TC activity (e.g., Camargo et al. 2004). In Figure 14 we show the differences between the 30-year mean values of these parameters from the 4CO2 and the PREIND case.

The tropical mean of the 4CO2-PREIND difference of the 700-hPa relative humidity (RH700) exhibits a very small increase, consistent with Held and Soden (2006). However, locally some considerable change is visible (Figure 14, upper panels). A substantial increase, for example, is found in the equatorial band of the Pacific ocean, whereas reductions are found the tropical Indian Ocean, subtropical Pacific and Atlantic oceans. In northern summer (left panel), the RH700 appears to decrease in the North Atlantic, whereas a very slight increased is found in the WNP region.

When averaged over the Tropics, the MPI difference (panels c and d) shows a reduction of this index. Consistent with Vecchi and Soden (2007b), the patterns of MPI change are similar to the patterns of SST change (Figure 7). MPI increases (decreases) over the region where the SST warming is more (less) intense. Thus, substantial increase of MPI is found in the equatorial Pacific and western Indian Ocean, while the index decreases over the southern Pacific, eastern Indian Ocean, WNP and tropical Atlantic, especially during northern summer (left panel).

The 4CO2-PREIND difference of the GP index (lower panels) reveals an increase of this parameter in the tropical Pacific, north of the equator, during northern summer. In most of the WNP sector, the difference is not statistically significant, though there is a portion of the region where the GP

exhibits a significant increment. The increase is more pronounced in the central-eastern North Pacific. Noteworthy, from the results shown in Section 4 (e.g., Figure 8), this is also the region where the TC activity does not appear to be reduced by the CO2 increase.

Overall, the results obtained from the parameters shown in Figure 14 are consistent with the findings we obtained with the TC tracking methods described in Section 2.4. The agreement appears to be particularly evident in the ATL region, where all of the empirical parameters suggest a reduction of the TC activity, consistent with the results shown in Section 4. In the WNP area, on the other hand, the agreement is less obvious. While the MPI shows a slight but visible decrease, the GP index exhibits some increment, especially in the eastern part.

6. Summary

In this study, a fully coupled high-resolution AOGCM has been used to investigate the possible impacts of greenhouse global warming on the characteristics of tropical cyclones. To our knowledge, this is the first time the impact of global warming on TCs is investigated by means of a state of the art fully coupled GCM.

The simulated TCs have many, basic, gross features similar to the observed ones. However, the rather low intensity of the low-level winds and the too large distance between the cyclone eye and the wind maximum remain unsatisfactory. These shortcomings are likely due to the model resolution, which, though rather high for long climate simulations, is still too coarse for an adequate representation of the tight structures accompanying these phenomena. Despite these problems, the model seems to be able to simulate a reasonable realistic climatology of TCs, both in terms of spatial distribution, seasonal and interannual variability of the TC activity. In particular, the model appears to capture at least some of the links between SST interannual variability and TC activity.

The enhanced concentration of atmospheric CO2 induces a warming of the entire tropical and subtropical upper ocean, accompanied by a redistribution of the tropical rainfall. The increase of the tropical ocean surface temperature, however, is not uniform, and the eastern Pacific exhibits a more pronounced warming with patterns that resemble El Niño SST anomalies. The total precipitation averaged over the Tropics increases with the CO2 increase, but the convective precipitation exhibits a significant reduction.

Along with the attenuated convective activity, our simulations show a substantial and significant reduction of the number of generated TCs, especially over the North West Pacific and North Atlantic tropical regions. Both the decrease in convective activity and and the reduced occurrence of TCs might be due to the larger potential energy barrier found when the CO2 concentration is increased. In the reduction of the TC activity in the ATL region, however, an important role appears to be played also by a considerable increase of the vertical wind shear.

The greenhouse warming is associated with a poleward expansion of the tropical warm SSTs. In particular, the 26°C isotherm, that appears to be crucial for the development of the TCs in the present climate, in the 4CO2 case migrates poleward of almost 10° latitude compared to the PREIND one. In the model, however, the warming of the subtropical and mid-latitudes is not accompanied by a poleward extension of the TC action, consistent with earlier works. The peaks of TC activity remain substantially confined equatorward of 20° latitude in both the Hemispheres.

Despite the reduced number of TCs generated when the CO2 has doubled and quadrupled, there is evidence of an increase in their intensity in terms of precipitation. This might be related with the increase of CAPE found in the warmer climate. The intensity of the simulated TCs expressed in

terms of near-surface wind (PDI) and surface pressure, on the other hand, does not appear to be significantly affected by the global warming. However, we think that this result might be actually related to the deficiencies that the model exhibits in reproducing realistic TC intensities.

Acknowledgment. The authors are indebted to Gabriel Vecchi, Chiara Cagnazzo and Andrea Alessandri for their precious help, useful suggestions and stimulating discussions. They also want to thank the three anonymous reviewers for their suggestions and constructive criticisms and K. Emanuel for making available the routines to compute the maximum potential index, MPI (http://wind.mit.edu/~emanuel/home.html). This work has been supported by the Euro-Mediterranean Centre for Climate Change and by the European Community project ENSEMBLES, contract number GOCE-CT-2003-505539.

References

Anthes R.A., Corell R.W., Holland G., Hurrel J.W., MacCracken M.C., and K.E. Trenberth, 2006: Hurricanes and Global Warming - Potential Linkages and Consequences. *Bull. Am. Meteor. Soc.*, DOI:10.1175/BAMS-87-5-617.

Aiyyer, A.R., and C. Thorncroft 2006: Climatology of vertical wind shear over the tropical Atlantic *J. of Clim.*, **19**, 2969-2983.

Behera S.K., J.J. Luo JJ, S. Masson, P. Delecluse, S. Gualdi, A. Navarra, T. Yamagata, 2005 Paramount impact of the Indian Ocean dipole on the East African short rains: A CGCM study. *J. of Clim.*, **18**, 4514-4530.

Bengtsson L., M. Botzet, M. Esch, 1995: Hurricane--type vortices in a general--circulation model. *Tellus-A*, **47**, 175-196.

Bengtsson L., M. Botzet, M. Esch, 1996: Will greenhouse gas--induced warming over the next 50 years lead to higher frequency and greater intensity of hurricanes? *Tellus-A*, **48**, 57-73.

Bengtsson L., K.I. Hodges, M. Esch, N. Keenlyside, L. Kornblueh, J.-J. Luo, and T. Yamagata, 2007: How may tropical cyclones change in a warmer climate? *Tellus-A*, **59**, 539-561.

Bister M. and K.A. Emanuel, 2002: Low frequency variability of tropical cyclone potential intensity. 1. Interannual to interdecadal variability. *J. Geophys. Res.*, **107**, 4801, doi:10.1029/2001JD000776.

Blanke B., P. Delecluse, 1993: Low frequency variability of the tropical Atlantic ocean simulated by a general circulation model with mixed layer physics. *J. Phys. Oceanogr.*, **23**, 1363-1388.

Broccoli A.J., and S. Manabe, 1990: Can existing climate models be used to study anthropogenic changes in tropical cyclone climate. *Geophys. Res. Lett.*, **17**, 1917-1920.

Camargo S.J., A.G. Barnston, and S.E. Zebiak, 2004: Properties of Tropical Cyclones in atmospheric general circulation models. IRI Tech. Rep. 04-02, International Research Institute for Climate Prediction, Palisades, N.Y. 72 pp.

Chan J.C.-L., 2000: Tropical cyclone activity over the western North Pacific associated with El Niño and La Niña events. *J. of Clim.*, **13**, 2960-2972.

Chauvin F., J.-F. Royer, and M. Deque, 2006: Response of hurricane-type vortices to global warming as simulated by ARPEGE-Climat at high resolution. *Clim. Dyn.}*, **27**, 377-399.

Chia H.H, and C.F. Ropelewski, 2002: The interannual variability in the genesis location of tropical cyclones in the northwest Pacific. *J. of Clim.*, **15**, 2934-2944.

Delworth T.L., and M.E. Mann, 2000: Observed and simulated multidecadal variability in the Northern Hemisphere *Clim. Dyn.*, **16**, 661-676.

De Maria, M, J.A. Knaff, and B.H. Connell, 2001: A Tropical Cyclone Genesis Parameter for the Tropical Atlantic. *Weath. Forec.*, **16**, 219-233.

Dutton, J. F., C. J. Poulsen, J. L Evans, 2000: The effect of global climate change on the region of tropical convection in CSM1. *Gophys. Res. Lett.*, **27**, 3049-3052.

Elsner J.B., and B. Kocher, 2000: Global tropical cyclone activity: A link to the North Atlantic Oscillation. *Geophys. Res. Lett.*, **27**, 129-132.

Emanuel K.A., 1987: The dependence of hurricane intensity on climate. *Nature*, **326**, 483-485.

Emanuel K.A., 2003: Tropical Cyclones. *Annu. Rev. Earth Planet. Sci.*, **31**, 75-104.

Emanuel K.A., and D.S. Nolan, 2004: Tropical cyclone activity and global climate. Preprints, *26th Conf. on Hurricanes and Tropical Meteorology*, Miami, FL., Amer. Meteor. Soc., 240-241.

Emanuel K.A., 2005: Increasing destructiveness of tropical Cyclones over the past 30 years. *Nature*, **436**, 686-688.

Fichefet T, M. A. Morales-Maqueda, 1999: Modelling the influence of snow accumulation and snow--ice formation on the seasonal cycle of the Antarctic sea-ice cover. *Clim. Dyn.*, **15**, 251-268.

Frank W.M., 1977: The structure and energetics of the Tropical Cyclone I. The Storm structure. *Mon. Wea. Rev.*, **105**, 1119-1135.

Frank W.M., and G.S. Young, 2007: The Interannual Variability of Tropical Cyclones. *Mon. Wea. Rev.*, **135**, 3587-3598.

Gent P.R., and J.C. McWilliams, 1990: Isopycnal mixing in ocean circulation models. *J. Phys. Ocean.*, **20**, 150-155.

Goldenberg S.B., C.W. Landsea, A.M. Mestas-Nunez, and W.M Gray, 2001: The recent increase in the Atlantic hurricane activity: causes and implications. *Science*, **293**, 474-479.

Goldenberg S.B., L.J. Shapiro, 1996: Physical mechanisms for the association of El Niño and west African rainfall with Atlantic major hurricane activity. *J. of Clim*, **9**, 1169-1187.

Gray W.M., 1968: Global view of the origin of tropical disturbances and storms. *Mon. Wea. Rev.*, **96**, 669-700.

Gray W.M., 1979: Hurricanes: Their formation, structure and likely role in the tropical circulation. *Meteorology over the Tropical Oceans*, D.B. Shaw (Ed.), Royal Meteorological Society, 155-218.

Gray W.M., 1984: Atlantic seasonal hurricane frequency .1. El-Nino and 30-mb Quasi--biennial oscillation influences. *Mon. Weather Rev.*, **112**, 1649-1668.

Gualdi, S., A. Navarra, E. Guilyardi, and P. Delecluse, 2003a: Assessment of the tropical Indo-Pacific climate in the SINTEX CGCM, *Ann. Geophysics*, **46**, 1-26.

Gualdi, S., E. Guilyardi, A. Navarra, S. Masina, and P. Delecluse, 2003b: The interannual variability in the tropical Indian Ocean as simulated by a CGCM. *Clim. Dyn.*, **20**, 567-582.

Gualdi, S., E. Scoccimarro, A. Navarra, 2008: Changes in Tropical Cyclone Activity due to Global Warming: Results from a High-Resolution Coupled General Circulation Model. *J. of Clim*. Vol. 21, pp. 5204-5228.

Guilyardi, E., P. Delecluse, S. Gualdi, and A. Navarra, 2003: Mechanisms for ENSO phase change in a coupled GCM, *J. of Clim.*, **16**, 1141-1158.

Haarsma R.J., J.F.B. Mitchell, C.A. Senior, 1993: Tropical disturbances in a GCM. *Clim. Dyn.*, **8**, 247-257.

Held I.M., and B.J. Soden, 2006: Robust responses of the hydrological cycle to global warming. *J. of Clim.*, **19**, 5686-5699.

Henderson-Sellers A, H. Zhang, G. Berz, K.A. Emanuel, W. Gray, C. Landsea, G. Holland, J. Lighthill, S.L. Shieh, P. Webster, and K. McGuffie, 1998: Tropical cyclones and global climate change: A post-IPCC assessment. *Bull. Am. Meteor. Soc.*}, **79**, 19-38.

Holland G.J., 1993: "Ready Reckoner" - Chapter 9, Global Guide to Tropical Cyclone Forecasting, WMO/TC-No. 560, Report No. TCP-31, World Meteorological Organization; Geneva, Switzerland.

Holland G.J., 1997: The maximum potential intensity of tropical cyclones. *J. Atmos. Sci.*, **54**, 2519-2541.

Knutson T.R., and R.E. Tuleya, 2005: Reply. *J. of Clim.*, **18**, 5183-5187.

Knutson T.R., and R.E. Tuleya, 2004: Impact of CO2 induced warming on simulated hurricane intensity and precipitation: sensitivity to the choice of climate model and convective parametrization. *J. of Clim.*, **17**, 3477-3495.

Knutson T.R., R.E. Tuleya, W. Shen, and I. Ginis, 2001: Impact of CO2-induced warming on hurricane intensities simulated in a hurricane model with ocean coupling. *J. of Clim.*, **14**, 2458-2468.

Knutson T.R., S. Manabe, 1995: Time-response over the tropical Pacific to increased CO2 in a coupled ocean atmosphere model. . *J. of Clim.*, **8**, 2181-2199.

Landsea C.W., B.A. Harper, K. Hoarau, and J. Knaff, 2006: Can we detect trends in extreme tropical cyclones?, *Science*, **313**, 452-454.

Landsea C.W., 2007: Counting Atlantic Tropical Cyclones Back to 1900. *EOS*, **88**, 197-202.

Latif M., N. Keenlyside, J. Bader, 2007: Tropical sea surface temperature, vertical wind shear, and hurricane development. Geophys. *Res. Lett.*, **34**, L01710.

Luo, J.-J., S. Masson, S. Behera, P. Delecluse, S. Gualdi, A. Navarra, and T. Yamagata, 2003: South Pacific origin of the decadal ENSO-like variation as simulated by a coupled GCM. *Geophys. Res. Lett.*, **30**, 2250, doi:10.1029/2003GL018649.

Madec, G., P. Delecluse, M. Imbard, and C. Levy, 1998: OPA 8.1 Ocean General Circulation Model reference manual, Internal Rep. 11, Inst. Pierre--Simon Laplace, Paris, France.

Masson, S., J.-J. Luo, G. Madec, J. Viala*f*rd, F. Durand, S. Gualdi, E. Guilyardi, S. Behera, P. Delecluse, A. Navarra and T. Yamagata, 2005: Impact of barrier layer on winter-spring variability of the southeastern Arabian Sea. Geophys. *Res. Lett.*, **32**, L07703, doi:10.1029/2004GL021980.

McDonald, R.E., D.G. Bleaken, D.R. Cresswell, 2005: Tropical storms: representation and diagnosis in climate models and the impacts of climate change. . *Clim. Dyn.*, **25**, 19-36, doi:10.1007/s00382-004-0491-0

Michaels P.J., P.C. Knappenberger, and C Landsea, 2005: Comments on "impacts of CO2-induced warming on simulated hurricane intensity and precipitation: Sensitivity to the choice of climate model and convective scheme". *J. of Clim.*, **18**, 5179-5182.

Mocrette J.J., 1991: Radiation and cloud radiative properties in the European centre for medium range weather forecasts forecasting system. *J. Geophys. Res.*, **96**, 9121-9132.

Nordeng T.E., 1994: Extended versions of the convective parametrization scheme at ECMWF and their impact on the mean and transient activity of the model in the Tropics. ECMWF Research Department, Technical Memorandum No. 206, October 1994, European Center for Medium Range Weather Forecasts, Reading, UK, 41 pp.

Oouchi K., J. Yoshimura, H. Yoshimura, R. Mizuta, S. Kusunoki, and N.A. Noda, 2006: Tropical cyclone climatology in a global-warming climate as simulated in a 20 km-mesh global atmospheric model: Frequency and wind intensity analyses. *J. Meteor. Soc. Japan*, **84**, 259-276.

Palmen, E., 1948: On the formation and structure of tropical hurricanes. *Geophysica*, **3**, 26-39.

Pezza A.B., and I Simmonds, 2005: The first South Atlantic hurricane: Unprecedented blocking, low shear and climate change. *Geophys. Res. Lett.*, **32**, L15712, doi:10.1029/2005GL023390.

Pielke Jr. R., C. Landsea, M. Mayfield, J. Laver, and R. Pasch, 2006: Reply to "Hurricanes and Global Warming - Potential Linkages and Consequences. *Bull. Am. Meteor. Soc.*, DOI:10.1175/BAMS-87-5-622.

Pielke Jr. R., C. Landsea, M. Mayfield, J. Laver, and R. Pasch, 2005: Hurricanes and Global Warming. *Bull. Am. Meteor. Soc.*, DOI:10.1175/BAMS-86-11-1571.

Rayner N.A., D.E. Parker, E.B. Horton, C.K. Folland, L.V. Alexander, D.P. Rowell, E.C. Kent, and A. Kaplan, 2003: Global analyses of sea surface temperature, sea ice, and night marine air temperature since the late nineteenth century. *J. Geophys. Res.*}, **108**, D14, 4407, doi:10.1029/2002JD002670.

Roeckner E, and Coauthors (1996) The atmospheric general circulation model Echam-4: model description and simulation of present-day climate. Max-Planck-Institut fur Meteorologie, Rep. No 218, Hamburg, Germany, 90 pp.

Roullet G., and G. Madec, 2000: Salt conservation, free surface, and varying levels: a new formulation for ocean general circulation models. *J. Geophys. Res*, **105**, 23927-23942.

Royer J.-F., F. Chauvin, B. Timbal, P Araspin, and D. Grimal, 1998: A GCM study of the impact of greenhouse gas increase on the frequency of occurrence of tropical cyclones. *Clim Dyn.*, **38**, 307-343.

Stevens B., 2005: Atmospheric Moist Convection, 2005. *Annu.Rev.Earth Planet.Sci.*, **33**, 605-43, doi:10.1146/annurev.earth.33.092203.122658.

Sugi M., A. Noda, N. Sato, 2002: Influence of global warming on tropical cyclone climatology: an experiment with the JMA global model. *J. Meteor. Soc. Japan*, **80**, 249-272.

Sugi M., and J. Yoshimura, 2004: A mechanism of tropical precipitation change due to CO2 increase. *J. of Clim*, **17**, 238-243.

Tiedtke M., 1989: A comprehensive mass flux scheme for cumulus parametrization in large-scale models. *Mon. Weather Rev.*, **117**, 1779-1800.

Timmermann R., H. Goosse, G. Madec, T. Fichefet, C Ethe and V. Dulie`re, On the representation of high latitude processes in the ORCALIM global coupled sea ice-ocean model, *Ocean Modell.*, **8**, 175-201, 2005.

Trenberth K., 2005: Uncertainty in Hurricanes and Global Warming. *Science*, **308**, 1753-1754.

Valke S, L. Terray, A. Piacentini, 2000: The OASIS coupled user guide version 2.4, Technical Report TR/ CMGC/00-10, CERFACS

Vecchi G.A., B.J. Soden, 2007a: Global Warming and the Weakening of the Tropical Circulation. *J. of Clim.*, **20**, 4316-4340.

Vecchi G.A., B.J. Soden, 2007b: Increased tropical Atlantic wind shear in model projections of global warming. *Geophys. Res. Lett*., **34**, L08702.

Walsh K.J.E, 1997: Objective detection of tropical cyclones in high--resolution analyses. *Mon. Weather Rev.*, **120**, 958-977.

Walsh K.J.E., and B.F. Ryan, 2000: Tropical cyclone intensity increase near Australia as a result of climate change. *J. of Clim.*, **13**, 3029-3036.

Walsh K.J.E., 2004: Tropical cyclones and climate change: unresolved issues. *Clim. Res.*, **22**, 77-83.

Watterson I.G., J.L. Evans, and B.F. Ryan, 1995: Seasonal and interannual variability of tropical cyclogenesis: Diagnostics from large-scale fields. *J. of Clim.*, **8**, 3052-3066.

Webster P.J., G.J. Holland, J.A. Curry, and H.-R. Chang, 2005: Changes in Tropical Cyclones Number, Duration and Intensity in a Warming Environment. *Science*, **309**, 1844-1846.

Willoughby H.E., J.A. Clos, M.G. Shoreibah, 1982: Concentric eye walls, secondary wind maxima, and the evolution of the hurricane vortex. *J. Atmos. Sci.*, **39**, 395-411.

Xie P., and P. Arkin, 1997: Global precipitation: A 17-year monthly analysis based on gauge observations, satellite estimates, and numerical model outputs. *Bull. Am. Meteor. Soc.*, **78**, 2539-2558.

Yoshimura J., M. Sigu, and A. Noda, 2006: Influence of greenhouse warming on tropical cyclone frequency. *J. Meteor. Soc. Japan*, **84**, 405-428.

CLIMATE SIMULATIONS AND SCENARIOS		
PREIND	Preindustrial ghg concentration	30 years
20C3M	20th Century ghg conc. + aerosols	30 years (1970-1999)
2CO2	2 x PREIND CO2 conc.	30 years
4CO2	4 x PREIND CO2 conc.	30 years

Table 1: Summary of the climate simulations used in this study.

NUMBER OF TCs 1970-1999		
	OBS	SXG 20C3M
TOT	2813	1986
MEAN	93.8	66.2
STD	10.9	9.2

Table 2: Total number of Tropical Cyclones found in the observations and in the 20th Century model simulation during the period 1970-1999.

		PREIND	2CO2	4CO2
T global mean	°K	288.37	290.377 (+2.01)	292.72 (+4.36)
T Tropics	°K	298.72	300.286 (+1.57)	302.41 (+3.69)
Prec. global mean	mm/day	2.757	2.809 (+1.89%)	2.852 (+3.45%)
Prec. Tropics	mm/day	3.317	3.353 (+1.09%)	3.354 (+1.12%)
ConvPrec global mean	mm/day	1.209	1.164 (-3.72%)	1.106 (-8.52%)
ConvPrec Tropics	mm/day	2.117	2.008 (-5.15%)	1.884 (-11.01%)

Table 3: Global average and tropical average of mean surface temperature, mean total precipitation and mean convective precipitation. The mean have been computed over the 30-year periods considered in the study. Values in parenthesis are the differences (absolute values for temperature and percentage for precipitation) with respect to the PREIND case.

	Number of Tropical Cyclones			Number of Tropical Cyclone Days		
	PREIND	2CO2	4CO2	PREIND	2CO2	4CO2
TOT	2196	1839	1229	5941	5085	3313
MEAN	73.2	61.3	41.0	198.0	169.5	110.4
STD	6.8	8.3	7.6	24.0	23.3	23.3

Table 4: Total number of TCs (left columns) and total number of TC days (right columns) found in the PREIND, 2CO2 and 4CO2 experiments. In all of the experiments a 30-year period is considered. In the upper row is the total number of TCs and TC days; in the middle row is the mean number of TCs and TC days per year; in the bottom row is the year-to-year standard deviation of the annual number of TCs and TC days. The average duration of the TCs, defined as the ratio between number of TC days and number of TCs, is 2.7 days for the PREIND, 2.8 for the 2CO2 and 2.7 for the 4CO2 experiment.

	PREIND	2CO2	4CO2
CAPE Tropical mean (J/Kg)	109.09	131.39 (+20%)	135.24 (+24%)
CAPE Tropical oceans only (J/Kg)	132.41	155.21 (+17%)	152.40 (+15%)
CIN Tropical mean (J/Kg)	13.06	16.04 (+23%)	18.73 (+43%)
CIN Tropical oceans only (J/Kg)	8.16	9.85 (+21%)	11.46 (+40%)

Table 5: Spatial average of mean convective available potential energy (CAPE) and mean convective inhibition (CIN). The mean CAPE and CIN are obtained by averaging over the 30-year periods of the PREIND, 2CO2 and 4CO2 experiments. The spatial average are computed over the whole tropical belt and over the tropical oceans only. Values in parenthesis are the percent increment with respect to the PREIND case.

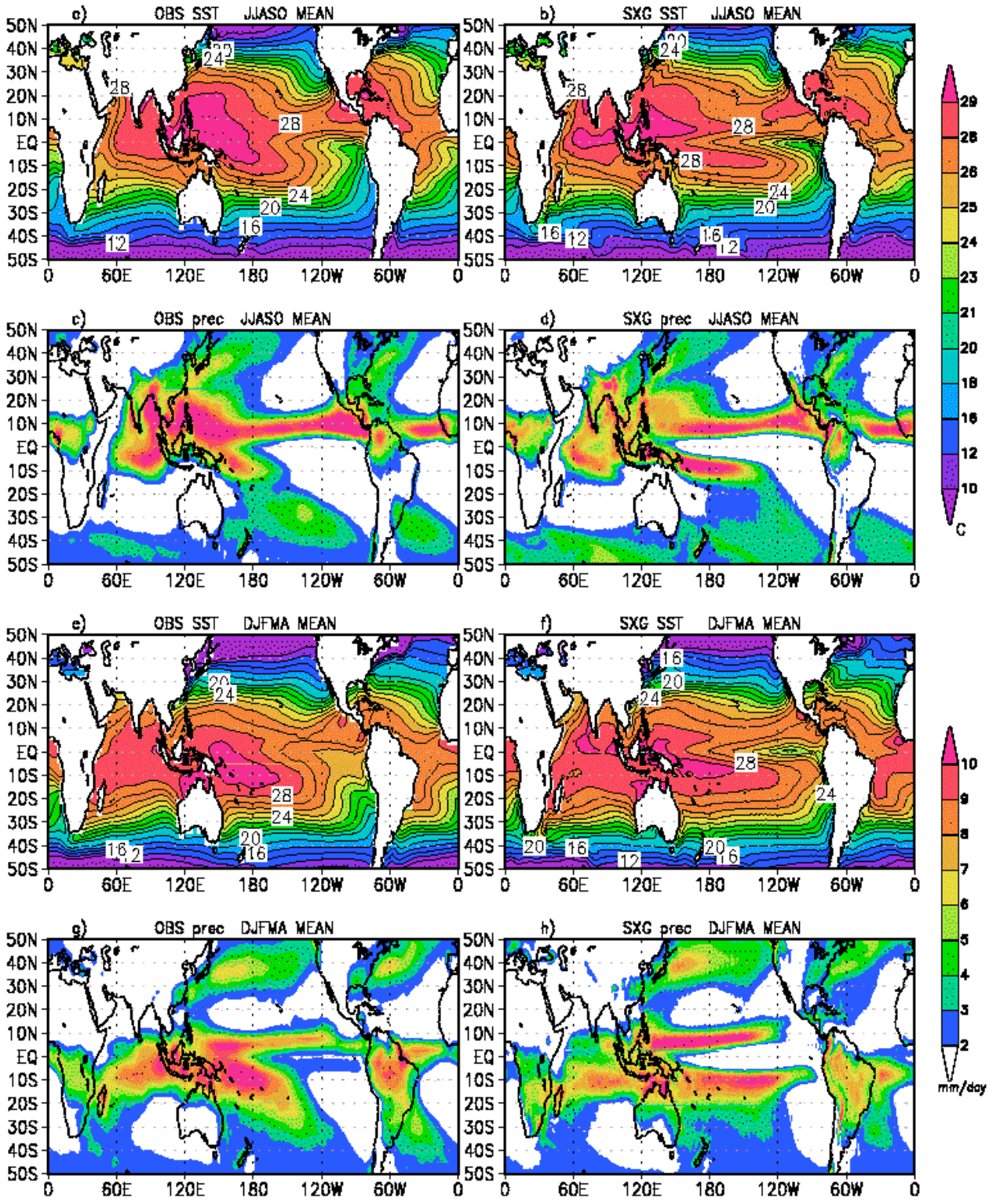

Figure 1: Seasonal means of sea-surface temperature (SST) and precipitation as obtained from the observations (left panels) and the model (right panels). The upper panels (a-d) show the extended Northern Hemisphere summer means June-July-August-September-October (JJASO); the lower panels (e-h) are the means obtained for the extended Southern Hemisphere summer December-January-February-March-April (DJFMA). The SST contours (panels a, b, e and f) are 2 °C. The precipitation contours (panels c, d, g and h) are 1 mm/day. Rainfall values lower than 2 mm/day are not plotted.

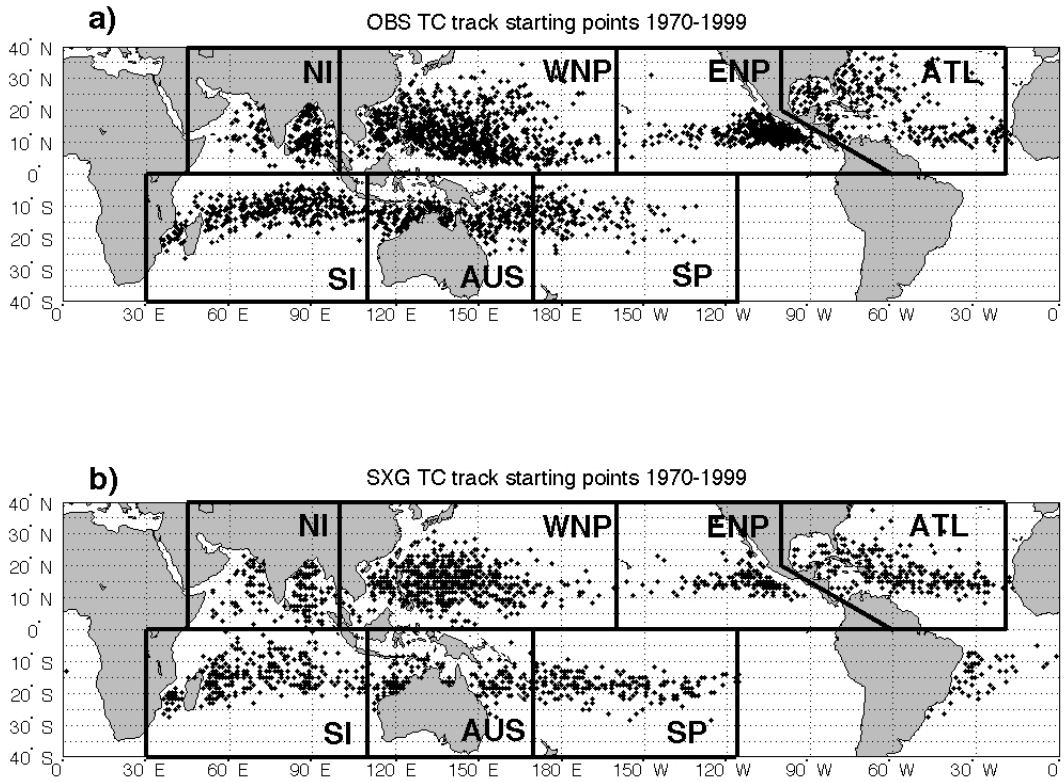

Figure 2: Distribution of the TC track starting points for the period 1970-1999 for the observations (panel a) and model (panel b). Each point corresponds to the geographical location of a TC at the time of its first detection. Following Camargo et al. (2004) seven regions of TC genesis have been defined. In the pictures these regions are delimited by thick black lines.

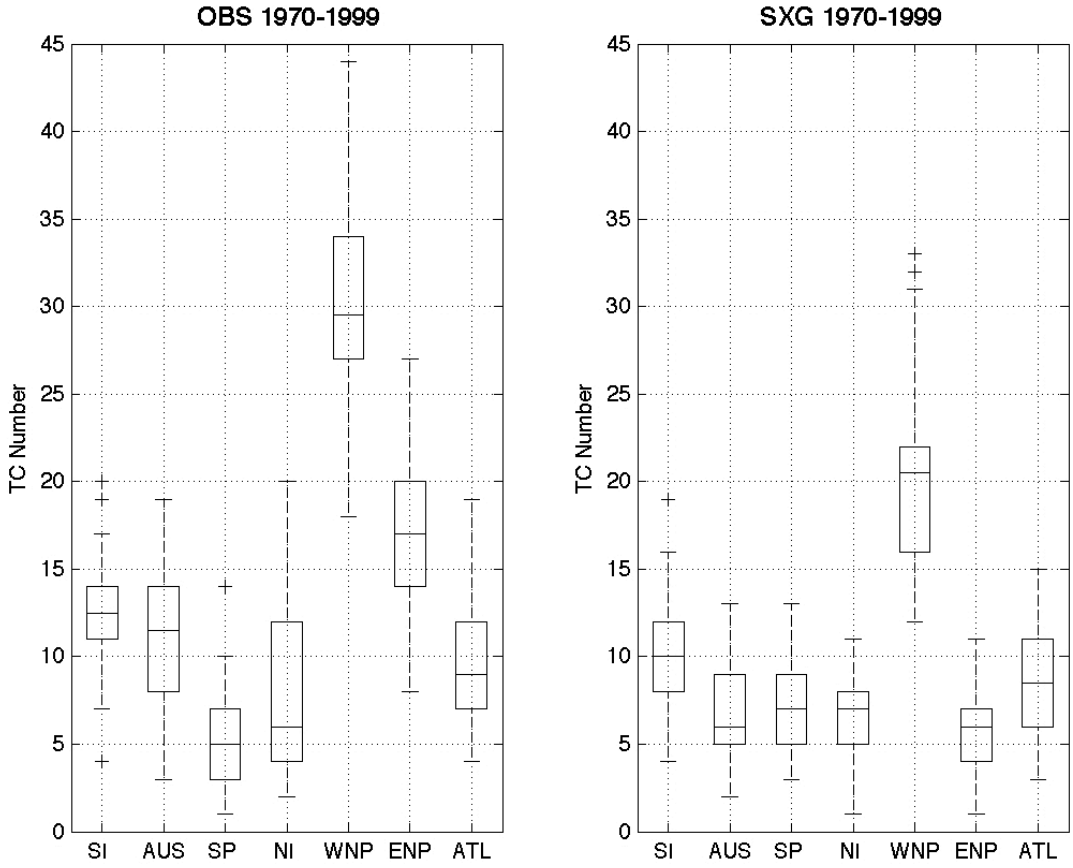

Figure 3: Box plots of the number of TCs per year for the observations (left panel) and model simulation (right panel). The number of TCs (y-axis) is plotted for each area of TC-genesis (x-axis) defined in Figure 4. In a box-plot, the box represents the interquartile (IQR) and contains the 50% of the data; the upper edge of the box represents the 75th percentile (upper quartile, UQ), while the lower edge is the 25th percentile (lower quartile, LQ). The horizontal lines within the box are the median. The vertical dashed lines indicate the range of the non-outliers. The values indicated with the crosses are the outliers, i.e. values that are either larger than UQ + 1.5 · IQR or smaller than LQ -1.5 · IQR.

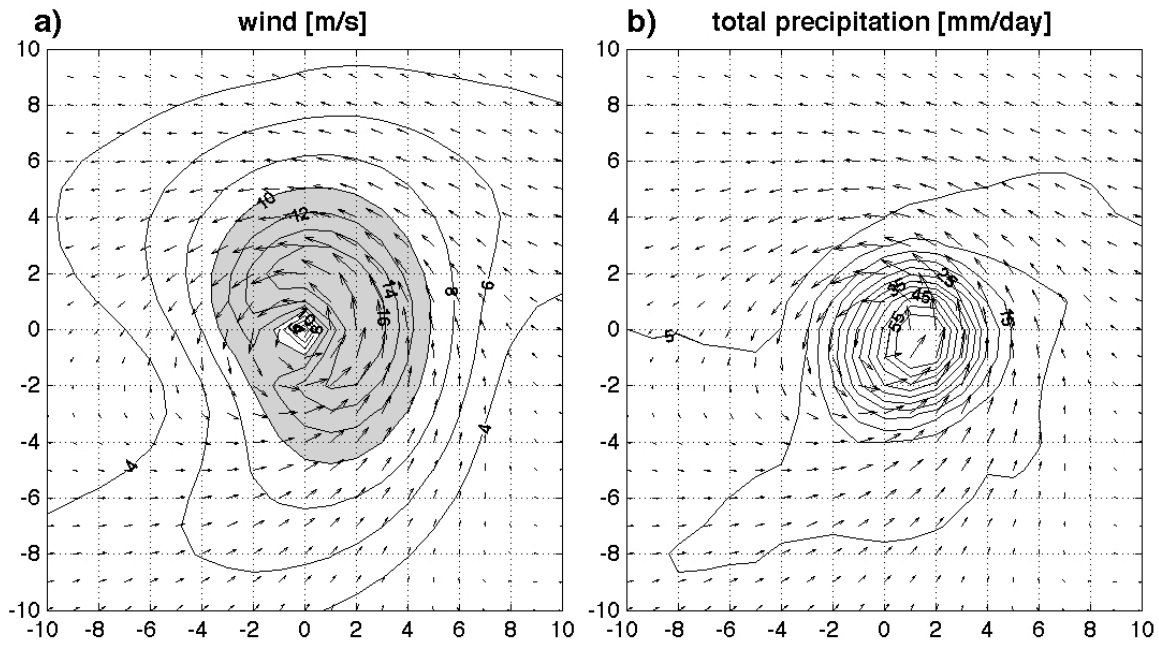

Figure 4: Composite patterns of 850-hPa wind and total precipitation associated with the simulated TCs. The composites have been computed by averaging the fields of the 100 most intense (in terms of precipitation) model TCs in the Northern Hemisphere. The fields have been averaged over the period of occurrence of the TCs and over the 100 events. The mean fields have been computed over a spatial domain centred in the core of the cyclone and extending 10º each side. In panel a) the of 850-hPa wind (arrows) is plotted along with the intensity of the wind (contour). The contour interval is 2 m/s. Contours larger than 10 m/s are shaded. Panel b) shows the 850-hPa wind (arrows) along with the total precipitation rate. The contour interval is 5 mm/day.

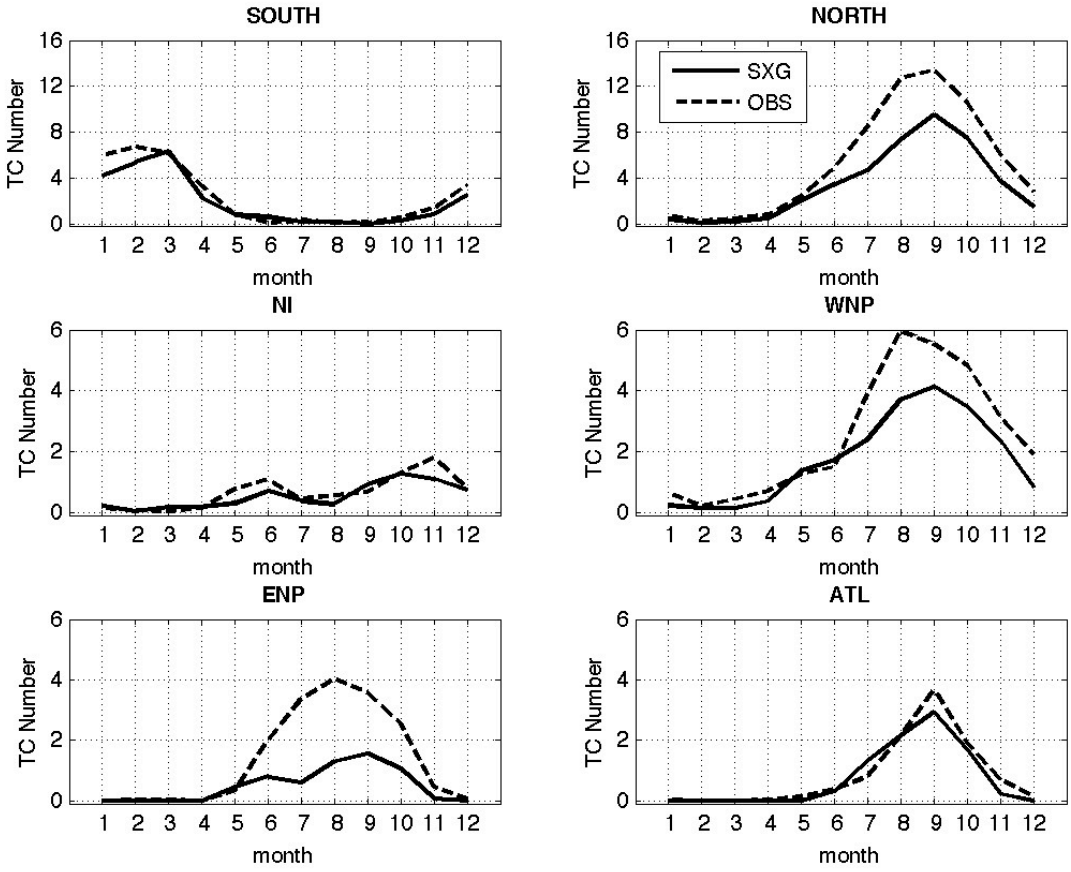

Figure 5: Seasonal modulation of the TC occurrence for the observations (dashed lines) and model simulation (solid lines) and for different region of the Tropics. Upper panels: tropical region of the Southern Hemisphere (left) and of the Northern Hemisphere (right). Middle and lower panels: northern Indian Ocean, western tropical Pacific, eastern tropical Pacific and tropical Atlantic.

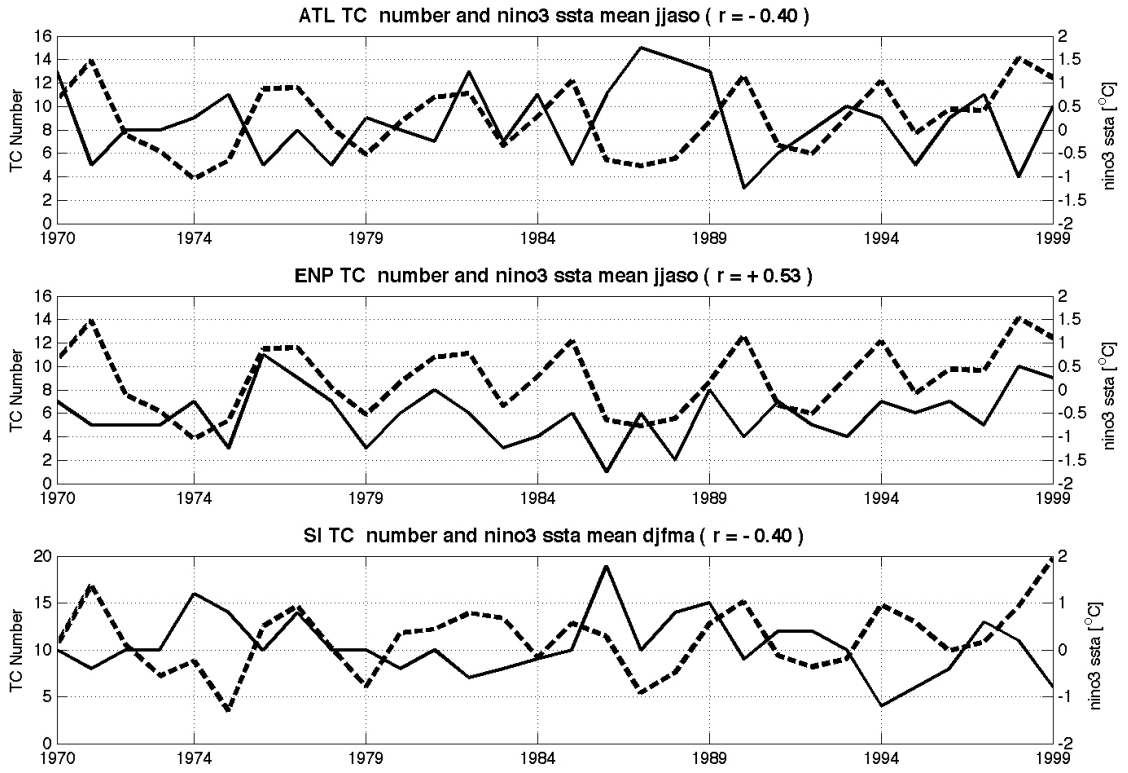

Figure 6: Time series of the number of TCs along with the NINO-3 index for different regions of the Tropics. The dashed lines show the interannual variation of the number of simulated TCs in the northern tropical Atlantic (upper panel), northern tropical eastern Pacific (middle) and Southern Indian Ocean (lower panel). The solid line show the value of NINO-3 SSTA index defined as the average of the SST anomaly over the NINO-3 region (5°S-5°N ; 150°W-90°W). The values of the NINO-3 index plotted in the ATL and ENP case have been obtained for JJASO, whereas for the SI case it has been computed for DJFMA. The value of the correlation between the two curves (r) is also shown.

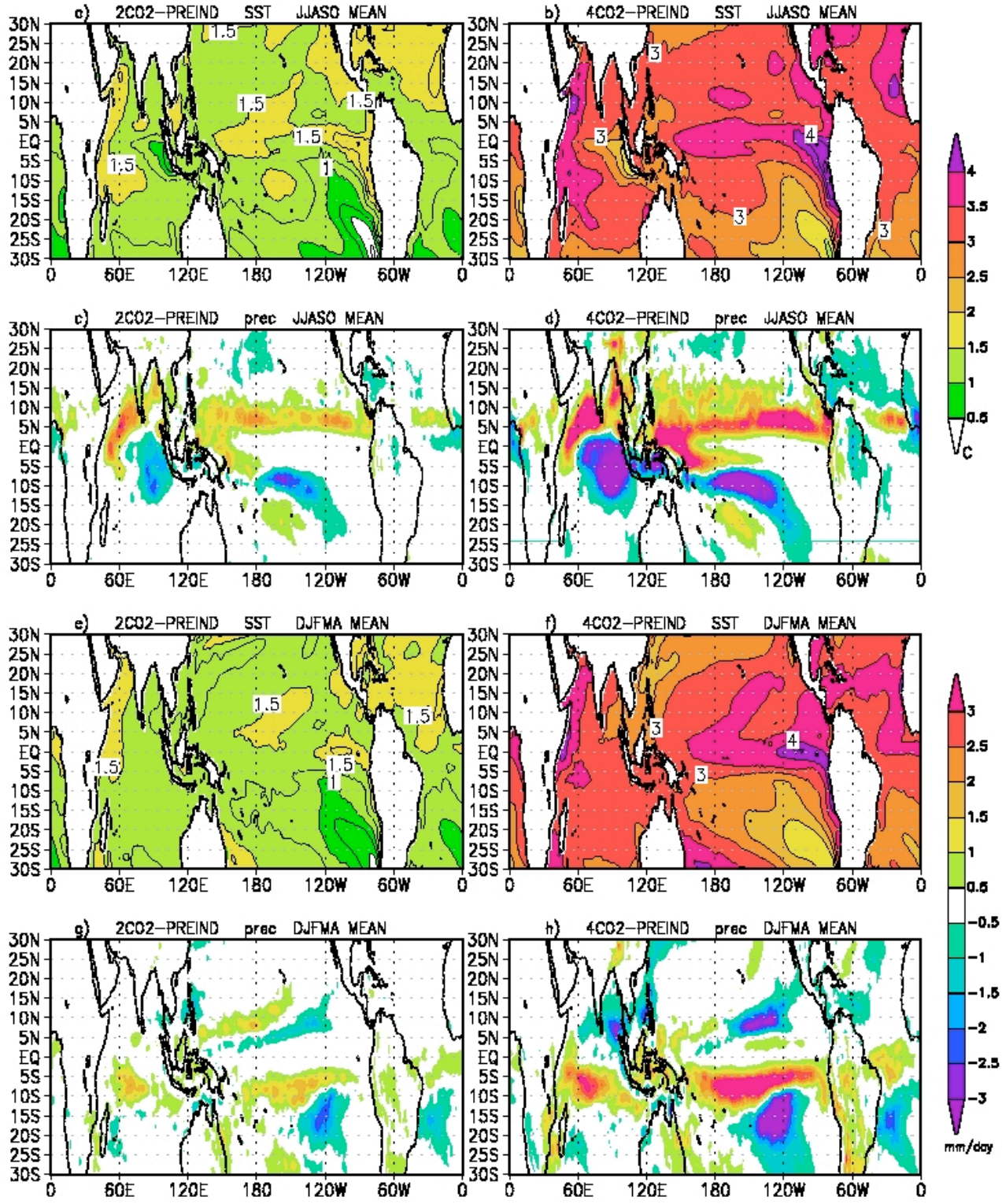

Figure 7: Differences between the seasonal mean SST and precipitation obtained from the 2CO2 and PREIND experiments (left panels) and 4CO2 and PREIND experiments (right panels). Panels a, b, e and f show the differences in mean SST; contour interval is 0.5 °C. Panels c, d, g and h show the differences in mean precipitation, with a contour interval of 0.5 mm/day.

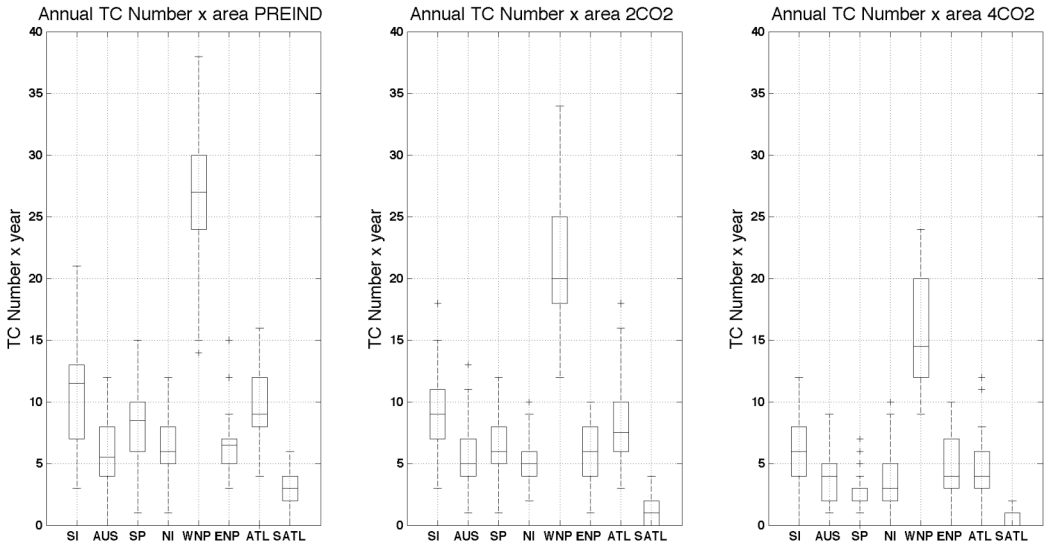

Figure 8: Box plot of the annual number of TCs in the areas defined in Figure 4 and for the tropical South-Atlantic (SATL) region. Left panel: PREIND experiment; middle panel: 2CO2 experiment; right panel: 4CO2 experiment.

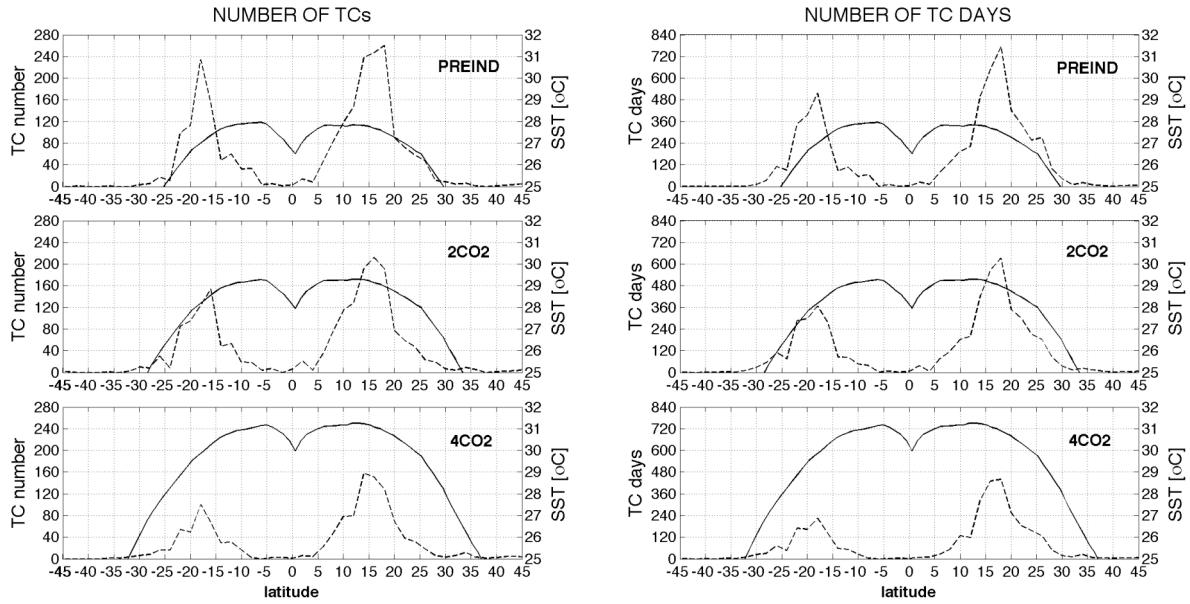

Figure 9: Latitudinal distribution of the total number of simulated TCs (left panels), TC days (right panels) and zonal mean value of SST for the PREIND experiment (upper panels), the 2CO2 case (middle panels) and the 4CO2 experiment (lower panels). On the x-axis is the latitude. The y-axis on the left show the number of TCs and TC days and on the right the SST value. The dashed curves show the meridional distribution of the total number of TCs and TC days, with maxima centred between 15° and 20° latitude in both the Hemispheres. The solid curves show the distribution of the zonal mean SST. The two curves indicate, for each latitude, the number of TCs and the number of TC days and the corresponding values of SST.

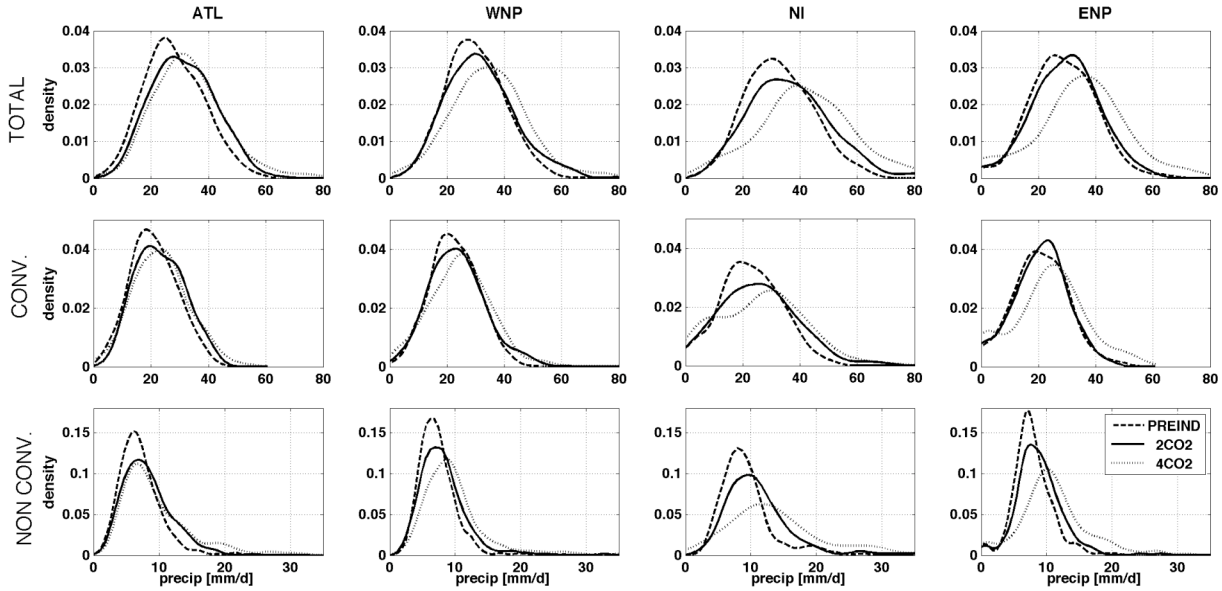

Figure 10: Probability density function (PDF) of total precipitation (upper row), convective precipitation (middle row) and large scale precipitation (bottom row) associated with the simulated TCs in the different regions for the PREIND case (dashed line), 2CO2 case (solid line) and 4CO2 experiment (dotted line). On the x-axis is the value of precipitation in mm/day. On the y-axis is the (density of) frequency of events corresponding to a certain amount of rainfall.

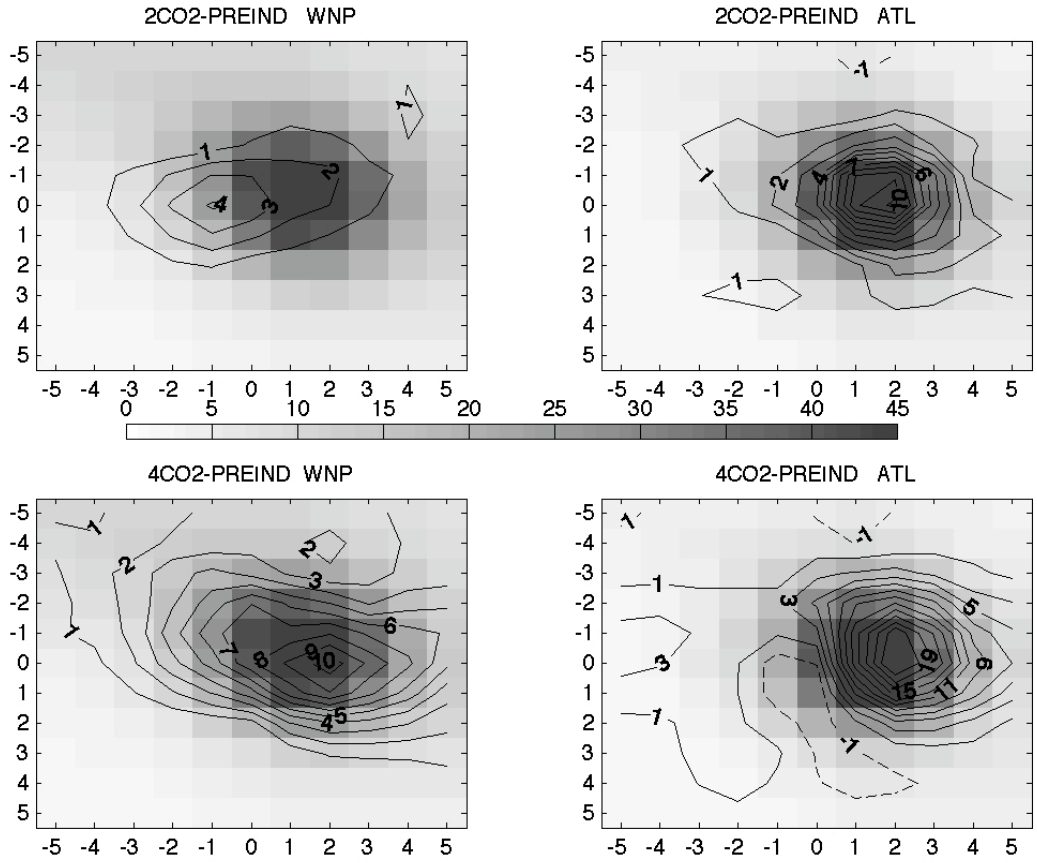

Figure 11: Left panels: composite of TC precipitation for the PREIND experiment over the WNP region (shaded pattern) along with the difference 2CO2-PREIND (upper panel) and 4CO2-PREIND (lower panel) shown by the contour patterns. The composites represent the mean rainfall rate averaged over the TC life time and over the number of TCs for the considered regions. The means have been computed for a domain centered on the core of the cyclones and extending 5º each side. Right panels: as for the left panels but for the ATL region. The PREIND rainfall composite (shaded patterns) have a shaded contour interval of 5 mm/day. The difference between the 2CO2 and PREIND composite and the 4CO2 and PREIND composite (contour patterns) have a contour interval of 1 mm/day. The contour lines show only the values that are statistically significant at a 95% level. The significance test has been performed using the boot-strap method.

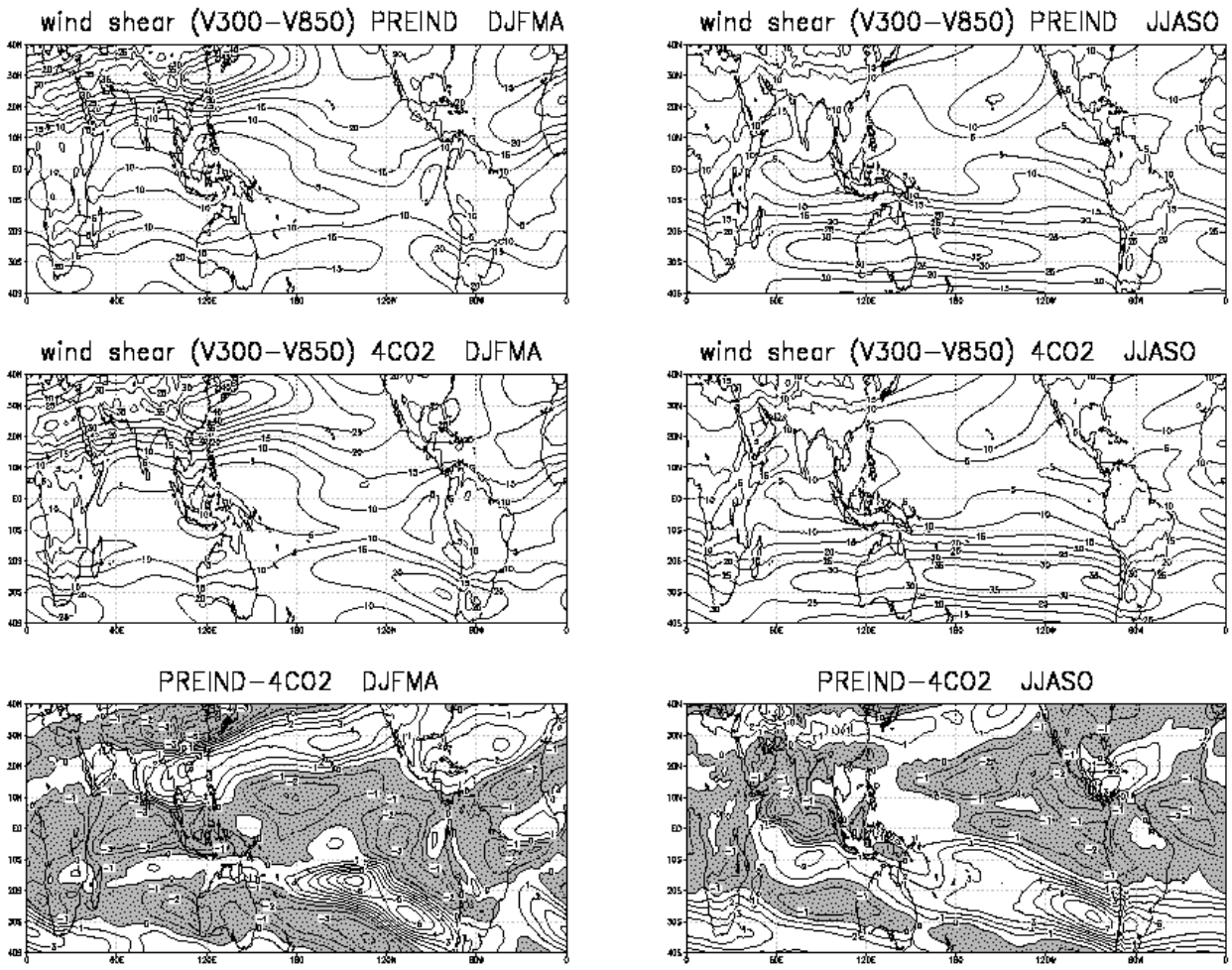

Figure 12: Seasonal mean of the vertical wind shear defined as the difference between the wind at 300 hPa and at 850 hPa (winds shear = sqrt{(u_{300}-u_{850})^2+ (v_{300}-v_{850})^2}). On the left panels are the results for the Southern Hemisphere extended summer (DJFMA), whereas on the right panels the values for the Northern Hemisphere extended summer (JJASO). The upper panels show the fields for the PREIND experiment. The middle panels the results from the 4CO2 experiments. For these plots, the contour interval is 5 m/s. The lower panels show the difference between the 4CO2 and the PREIND case. For these plots the contour interval is 1 m/s and negative values are shaded.

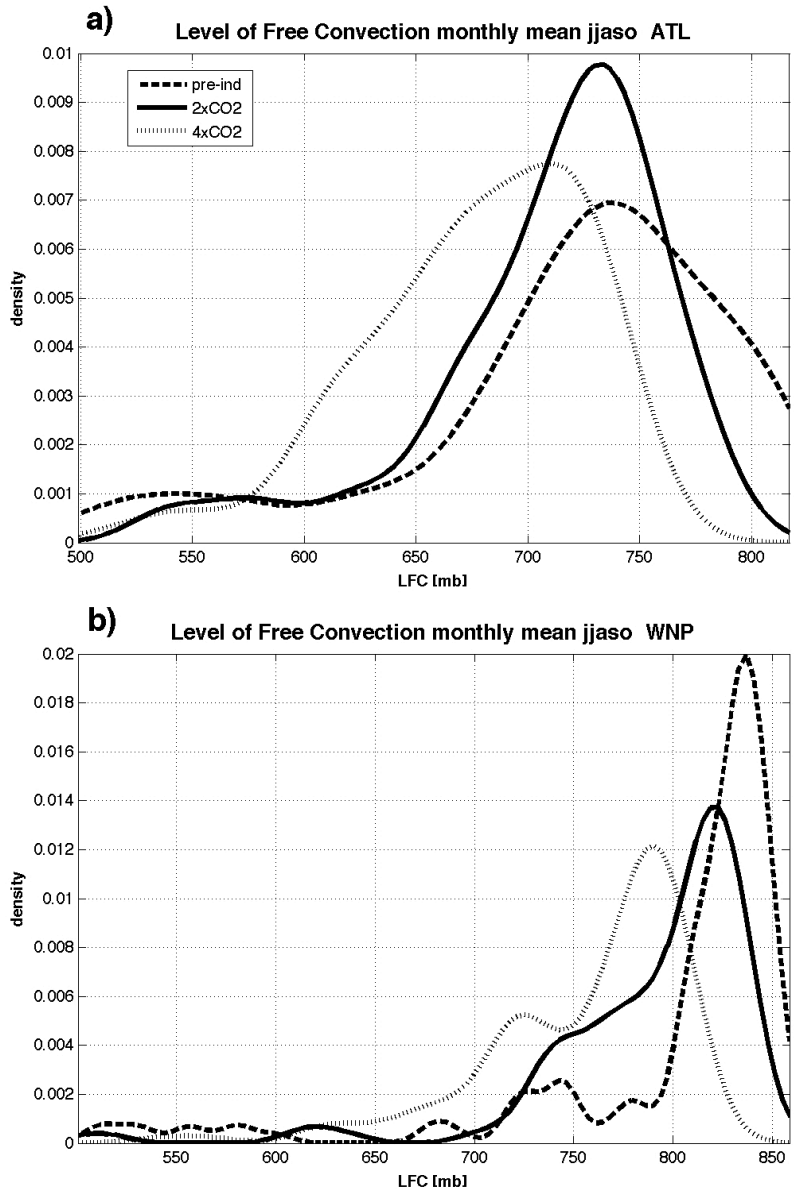

Figure 13: Probability density function (PDF) of the level of free convection (LFC) for the PREIND case (dashed), the 2CO2 case (solid line) and the 4CO2 experiment (dotted curve) over the ATL region (panel a) and the WNP region (panel b) during northern summer (JJASO). On the x-axis is the value of vertical levels in Millibar (mb), and on the y-axis is the (density of) frequency of occurrence at which free convection can be triggered at that level.

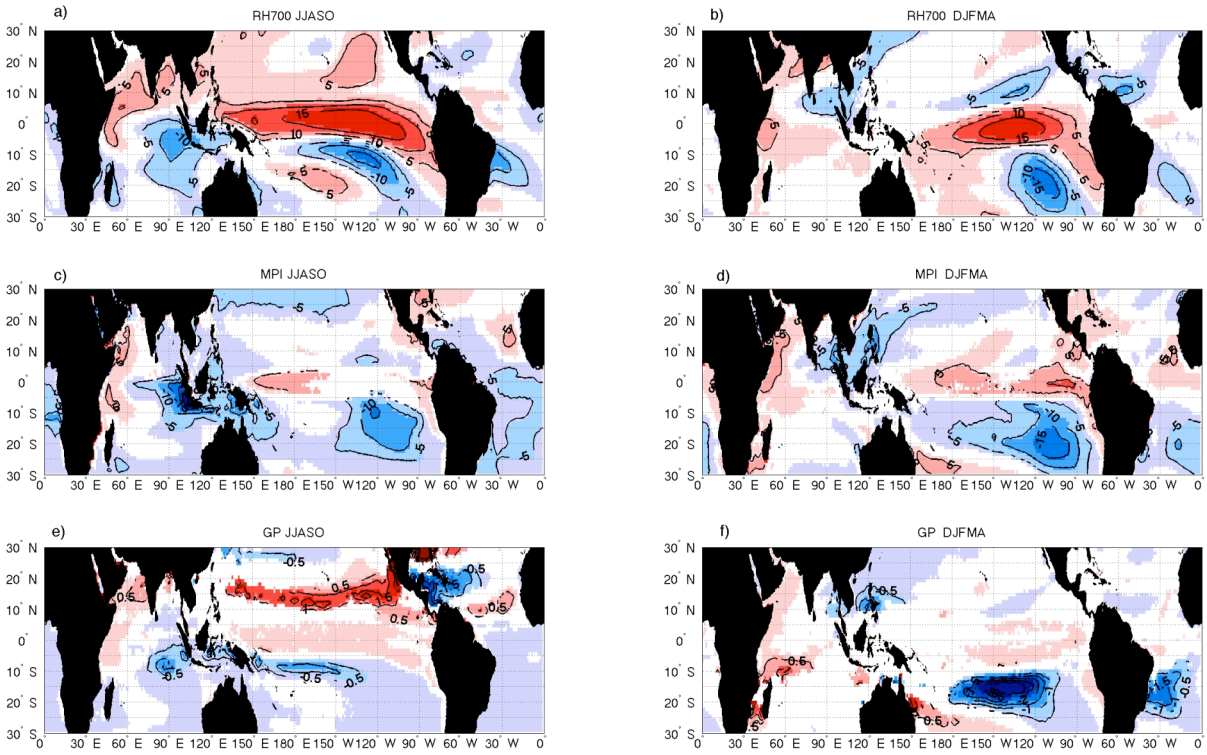

Figure 14: 4CO2-PREIND differences of the mean values of 700-hPa relative humidity (RH700, panels a and b); maximum potential index (MPI, panels c and d) and genesis potential index (GP, panels e and f). Left panels: northern summer; right panels: northern winter. The RH is expressed in %, the MPI in m/s and the GP index in (number of TC)/(unit area x decade). Only statistically significant at a 95% level contours are shown. The significance test has been performed using the boot-strap method.